University of Granada
Faculty of Science

The work presented to obtain the title of
DOCTOR OF PHILOSOPHY

Martin Jelínek
Instituto de Astrofísica de Andalucía CSIC

STUDY OF GAMMA-RAY BURSTS USING ROBOTIC TELESCOPES

Director de la tesis: Alberto J. Castro-Tirado, PhD.
Programa del estudio: Métodos y Técnicas Avanzadas en Física

Granada 2007

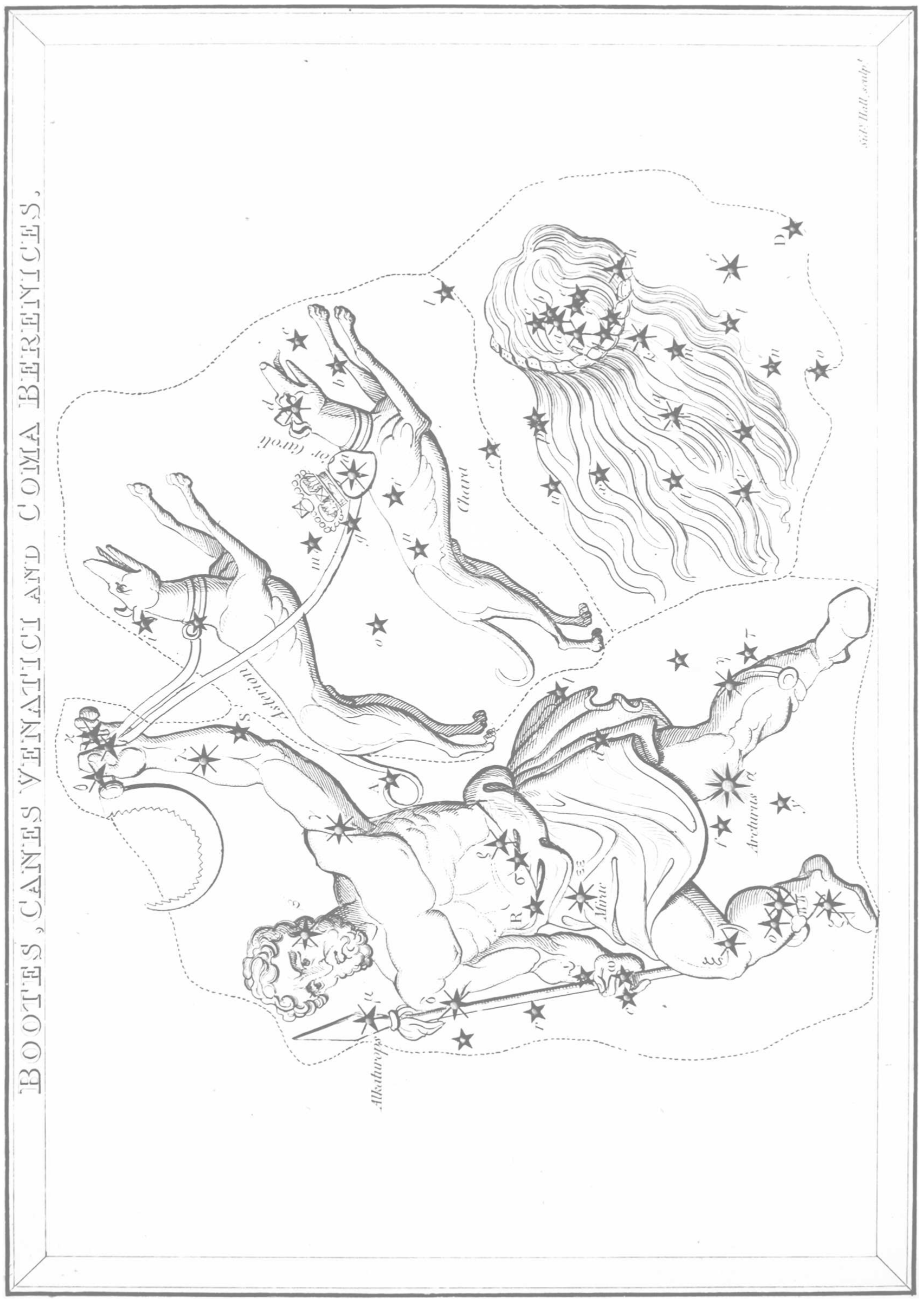
BOOTES, CANES VENATICI AND COMA BERENICES,
Alkaturops
Arcturus
Mirac
Asterion
Chara
Cor Caroli
Sid. Hall, sculp.

The study of Gamma Ray Bursts with robotic telescopes

Martin Jelínek

Instituto de Astrofísica de Andalucía, CSIC

3.9.2007

Abstract

This work talks about gamma-ray bursts (GRBs), observed as brief flashes of gamma radiation of cosmic origin. The phenomena, now considered one of the most energetic phenomena in the Universe, was discovered in 1967.

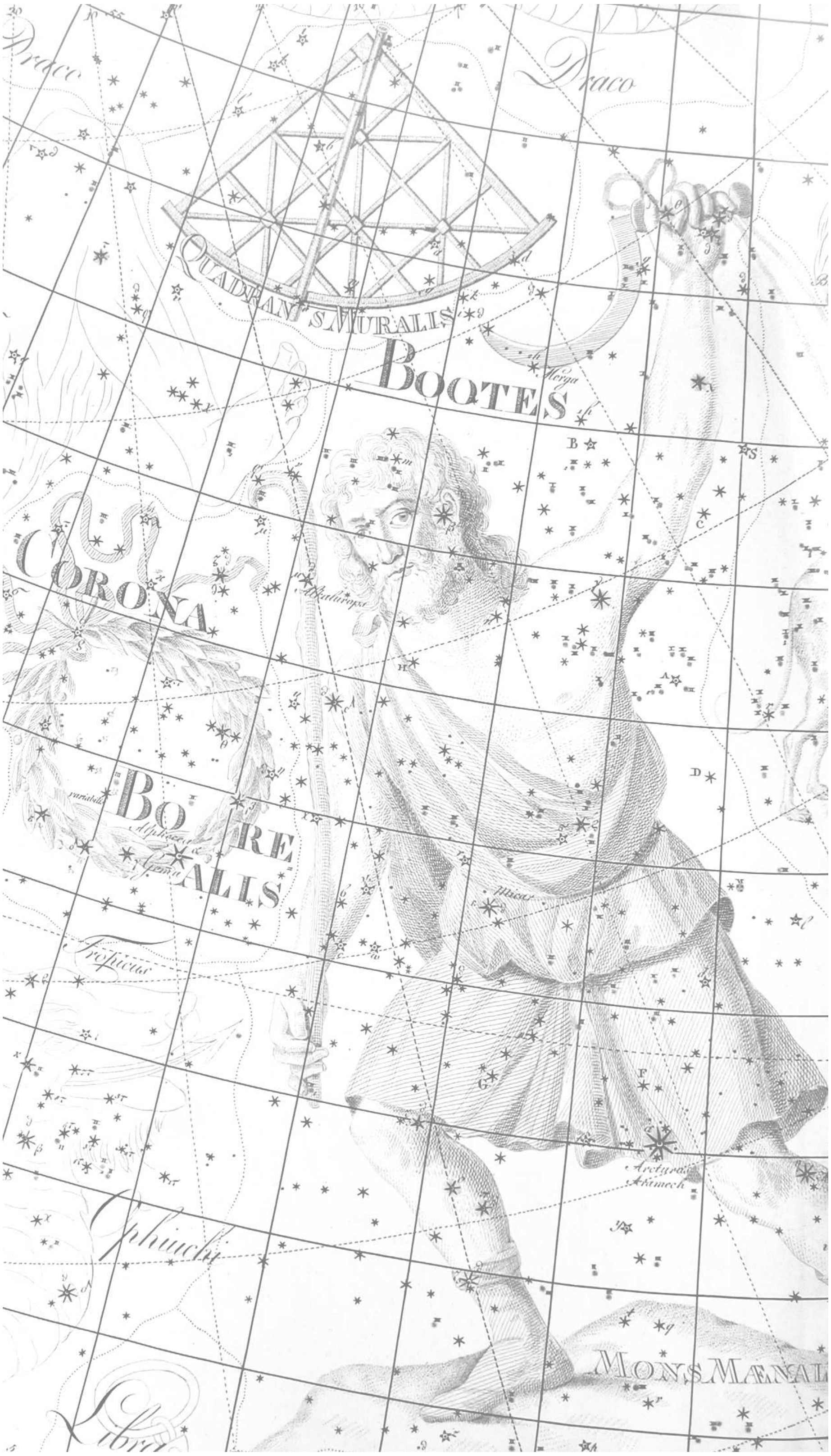
Draco
Draco
QUADRANS MURALIS
BOOTES
CORONA
BOREALIS
Tropicus
Ophiuchi
MONS MÆNALI
Libra
Arcturus

INDEX

re stellam unã. In utroqꝫ humero singulas. In utroqꝫ mãma sin-
gulas. sed clariorẽ dextrã: ⁊ sub ea alterã obscurã: ⁊ i cubito dextro
clarã unã. In zona unã clarꝰ ceteris lucentẽ. hec stella arcturꝰ ap-
pellatᷣ. In utrisqꝫ pedibꝰ singulas: que oĩo sunt quatuordecim.

Boetes

Coronã humero sinistro prope contingere arctophi-
lax videtᷣ: que ante engonasin dextri pedis calce cõ-
iungit. hec cancro ⁊ leone exoriẽte occidere: cũ scor-

I. The bright optical flash from GRB 060117

A bright long-soft GRB 060117 was detected by *Swift* satellite on January 17, 2006, at 6:50:01.6 UT. It showed a multi-peak structure with T_{90}=16 ± 1 s with maximum peak flux 48.9 ± 1.6 ph $cm^{-2}s^{-1}$. Coordinates computed by *Swift* were available within 19 s and immediately distributed by GCN [6].

FRAM received the notice at 06:50:20.8 UT, 19.2 s after the trigger and immediately started the slew. The first exposure started at 06:52:05.4, 123.8 s after the GRB. Eight images with different exposures were taken before the observation was terminated. A bright, rapidly decaying object was found, and its presence was reported by [12] and [10] soon after the discovery. The point-spread function of the object is similar to the stars in the image, and the object did not move more than 2′′ over the course of our observation, ruling out a near-Earth object crossing the field of view. The weather conditions during the observation were very good, but the Moon was nearly full (93 %) and the GRB location was only slightly more than 5° above the horizon. Consequently, the magnitude limits of our observation were ~ 2.5 mag worse than the technical limit of the FRAM instrument in the optimal conditions. Table 1 displays the log of our observations (see also Fig 1), where the magnitude errors do not include systematic error of the USNO-B1.0 R1 magnitude, which should be <0.1 mag.

An optical counterpart to GRB 060117 was found 128.8 s after the burst at

$$\alpha = 21^{h}51^{m}36\overset{s}{.}23 \quad \delta = -59^{\circ}58'39\overset{''}{.}3 \quad \pm 1\overset{''}{.}5 \quad \text{(J2000)}.$$

The error amounts to a 1-σ uncertainty including systematic errors.

1.1 Follow-up

Swift itself could not observe the GRB with its X-ray and optical instruments, because of the Sun observing constraint [5]. One month later on Feb 14 and 15, 2006, *Swift* XRT [4] pointed to the burst position and did not detect any source at the corresponding position with a 3-σ limit of 1.0×10^{-3} counts s^{-1}, corresponding to an unabsorbed 0.2 – 10 keV flux upper limit of 2.3×10^{-14} erg cm^{-2} s^{-1}. The burst was also detected by Konus-Wind [8] and by Suzaku WAM [26].

Unfortunately, the later optical follow-up was unsuccessful due to cloudy weather in both New Zealand and South Africa. The limits reported by PROMPT [16] (observations beginning 18.0 h after the burst), however, suggest a surprisingly rapid decay. The search for a radio afterglow was also unsuccessful [21].

The lag-luminosity pseudo-redshift estimation from *Swift* data yields $z \simeq 1.3 \pm 0.3$ [6]. The redshift estimate based on the γ-ray data from Konus-Wind gives $z \simeq 0.45\pm0.2$ [17].

1.2 Host galaxy identification and redshift estimation

Further observation was performed on the field of GRB060117 during the following year, leading to the discovery of the host galaxy and, this being observed in multiple filters could lead to the redshift estimation. TBF

1.3 Data acquisition and reduction

FRAM is part of the Pierre Auger cosmic-ray observatory [18], and its main purpose is to immediately monitor the atmospheric transmission. FRAM works as an independent, RTS2-driven [11], fully robotic system, and it performs a photometric calibration of the sky on various UV-to-optical wavelengths using a 0.2 m telescope and a photoelectric photomultiplier. As a primary objective, FRAM observes a set of chosen standard stars and a terrestrial light source. From these observations it obtains instant extinction coefficients and the extinction wavelength dependence. Additionally, FRAM is able to follow GCN alerts, using its wide-field camera with a fixed *R*-band filter.

The wide-field camera consists of a Carl Zeiss Sonnar 200 mm $f/2.8$ telephoto lens, SBIG ST7 imager, and Bessel R-band filter. The ST7 camera has a 768×512 Kodak KAF-0402E CCD that covers a field of view of $120' \times 80'$ with a scale of $9\farcs6$/pixel. The effective diameter of the lens is 57 mm and the 3σ limiting magnitude under optimum

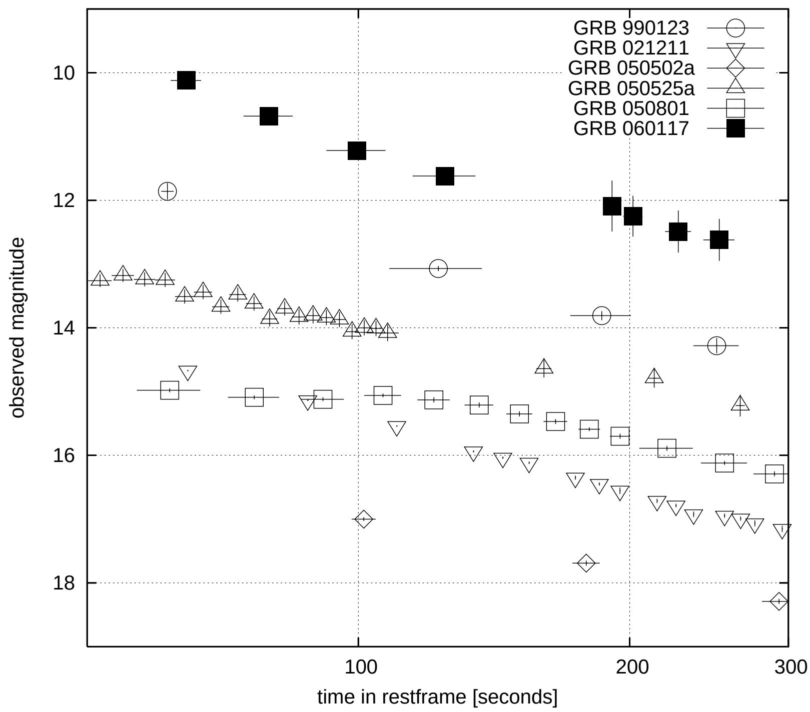

Figure 1: The optical light curve of GRB 060117 in comparison with other well-covered early GRB optical emissions: GRB 990123 [1], GRB 021211 [14], GRB 050502a [9], GRB 050525a [3], and GRB 050801 [19]. In this figure we use $z \approx 1.0$ for GRB 060117. Observed *R*-band magnitudes are shown, except for GRB 050525a, where the *V*-band values are plotted.

Table 1: Optical R-band photometric observations of the optical flash GRB 060117. The magnitudes are not corrected for Galactic extinction ($A_R \sim 0.01$ mag). $T - T_0$ is mean exposure time since the GRB.

UT Date of exp. start	$T - T_0[s]$	$T_{\mathrm{exp}}[s]$	R	δR
2006 Jan. 17.786169	128.8	10	10.12	0.13
2006 Jan. 17.786833	159.1	20	10.68	0.12
2006 Jan. 17.786343	199.3	30	11.22	0.14
2006 Jan. 17.787583	249.7	40	11.62	0.18
2006 Jan. 17.789109	382.4	10	12.09	0.45
2006 Jan. 17.789410	403.4	20	12.25	0.36
2006 Jan. 17.789815	452.9	30	12.49	0.37
2006 Jan. 17.790336	502.9	40	12.62	0.37

conditions reaches $R \sim 15.0$ for a 30 s exposure.

The raw images were dark-frame subtracted using a median of several dark-frame exposures. Given the significant dark current of the camera, the darks were treated separately for each exposure time. The flat-field correction was then applied using the median of 40 normalized 1s exposures obtained while mosaicing through the twilight sky. The aperture photometry was done using the `phot` routine in IRAF[1] with the aperture diameter of 2 pixels. To get a precise astrometric position of the source, we used the four most significant images and computed the average position.

The images were astrometrically and photometrically calibrated on the fly using the `past` program in the context of JIBARO [7], using all sources with more than 10-σ significance from the image compared to USNO-B1.0 [15] positions and *R1* magnitudes. `Past` employs a sigma-clipped third-degree polynomial surface fit. For the astrometry, an error-weighted mean of the zero point is used. Systematic errors of USNO-B1.0 should be less than $0\farcs2$ in the astrometry and less than 0.1 mag for the photometry. Since the Galactic extinction, taken from the maps published by [20] is very low ($E_{B-V} = 0.038$), we neglect this value in the following discussion.

1.4 Discussion

In the search for the interpretation of the lightcurve, we assume a uniform ISM, and that the influence of the internal shock emission on the lightcurve is negligible because our observation starts ~100 s after the end of the gamma-ray burst.

In the simplest case, the lightcurve can be fitted and a single power law with a temporal flux-decay index $\alpha = -1.73 \pm 0.12$. The $\chi^2/d.o.f.$ for this fit is 1.296. If we assume this decay to be a signature of a pure forward shock, we get the value of the electron energy distribution power-law index $p = 3.3 \pm 0.1$. This value is very high in comparison with other known optical transients, but it is consistent with $p = 3.82^{+1.0}_{-0.5}$ as computed from the Konus-Wind spectra of the GRB [8] [cf. 23]. In contrast, if the linear decay is a signature of a pure reverse shock, we get $p = 2.0 \pm 0.1$ – close to the typical value for the optical transients observed so far. We should note that such a reverse shock emission should be accompanied by a forward shock with $\alpha_F \simeq$-0.7.

Another possibility [after 22] is to interpret the data as a Type I lightcurve [as given by 27], which depicts a transition between the reverse and the forward shock with

[1] IRAF is distributed by the National Optical Astronomy Observatory, which is operated by the Association of Universities for Research in Astronomy, Inc., under co-operative agreement with the National Science Foundation.

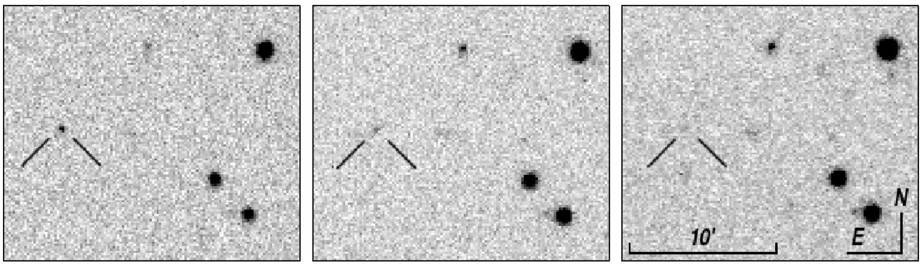

Figure 2: Details of the surroundings of the optical flash of GRB 060117 as observed by FRAM. Images taken 129, 249, and 480s after the trigger.

the passage of the typical frequency break ν_m through the observed passband at time $t_{m,f}$. We assume the lightcurve is initially dominated by a rapidly falling reverse-shock emission with $F_{\nu,r} \sim t_d^{-(27p+7)/35}$, followed by a forward-shock emission that rises as $F_{\nu,r} \sim t_d^{+1/2}$ before $t_{m,f}$ and then decays with $F_{\nu,f} \sim t_d^{-(3p-3)/4}$. Using a χ^2 minimization fit to this scenario, we obtain $p = 2.96 \pm 0.06$, a magnitude of forward shock maxima $m_{m,f} = 11.82 \pm 0.04$, a time of the maxima $t_{m,f} = 301 \pm 4$ s (after trigger), and a magnitude of the reverse shock at $t = t_{m,f}$ $m_{m,r} = 12.43 \pm 0.05$ ($\chi^2/d.o.f.$ for this fit is 0.015). Corresponding decay indices are $\alpha_{\rm R}$=2.49±0.05 and $\alpha_{\rm F}$=1.47±0.03 (see Fig 3). If the crossing time $t_\times$ [27] coincides with the end of the GRB (i.e. ∼ 20 s), then we can estimate the peak magnitude of this OT as $R \sim 5$ mag by backward extrapolation.

Note, that this is only one of the plausible interpretations. There may be other possible explanations for this behaviour including density jump in the media [13] or energy injection [2]. Without a multiwavelength observation it is impossible to distinguish which of these possibilities actually took place.

The position of the burst and its distance from the Sun made the object difficult to observe. PROMPT [16] shows that the bright OT decayed very fast, and 20 hours after the burst its magnitude was already $I > 21.2$. Using the procedure of [24] we transform this limit to the filter of our observation: $R \gtrsim 21.5$ From this limit we then get the estimate of an average late decay as $\alpha_{\rm late} < -1.62$. Among the three interpretations we have shown, only the pure forward shock scenario is compatible with this limit without introducing an unusually early jet break, which is required to explain the other two scenarios.

Soon after the *Swift* trigger, a suspicion of an extremely low-redshift GRB was raised [25] due to the presence of a nearby galaxy PGC 128172 with $z = 0.04$ in the *Swift* errorbox. However, this discovered transient lies $3\overset{\rm m}{.}1$ from this galaxy, accordingly the projected distance – 160 kpc – is approximately four times larger than the visible major diameter of this galaxy. Furthermore, the position angle of the transient with respect to the PGC 128172, which we observe practically edge-on, is 97°. The association of the OT with this galaxy is, therefore, quite unlikely.

1.5 Conclusions

The GRB 060117 is the most intense (in terms of peak flux) GRB detected so far by Swift. With the maximum brightness of $R = 10.1$ mag, FRAM has discovered one of the optically brightest prompt optical emissions ever detected. The initial optical decay was found to be one of the steepest of an early GRB optical afterglow observed.

We have presented 3 scenarios for explaining the lightcurve. The apparent change

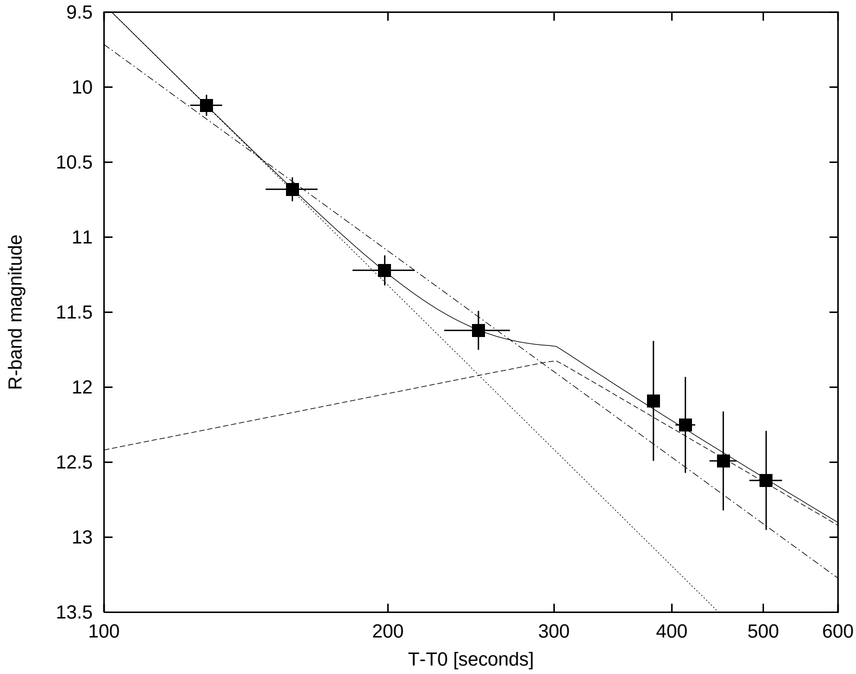

Figure 3: The R-band afterglow lightcurve of GRB 060117. The lightcurve is fitted as a superposition of reverse shock (dotted line) and forward shock (dashed line). The linear fit is plotted by a dot-and-dash line.

in its slope is neglected in two simple scenarios, where we suppose the observed lightcurve to only be the trace of a forward, resp. reverse, shock. In the third (preferred) scenario, the shape of the lightcurve is explained as a transition between reverse and forward shock emission. The forward-shock-only interpretation is flawless regarding the PROMPT limit, but shows rather spurious value of p. The other two scenarios (i.e. those involving reverse shock) result in a relatively slowly decaying forward shock, and later limits require an early jet break $t_j \sim 0.2$ d. The detailed analysis of this problem is beyond the scope of this letter.

Progress in further study of the particular case of GRB 060117 depends on the measurement of its distance. Therefore the follow-up and identification of host galaxy with a large telescope is of high importance.

A larger sample of GRB rapid follow-ups is needed to decide whether this kind of transition, already suggested for other bursts, is common.

References

[1] C. Akerlof, R. Balsano, S. Barthelmy, J. Bloch, P. Butterworth, D. Casperson, T. Cline, S. Fletcher, F. Frontera, G. Gisler, J. Heise, J. Hills, R. Kehoe, B. Lee, S. Marshall, T. McKay, R. Miller, L. Piro, W. Priedhorsky, J. Szymanski, and J. Wren. Observation of contemporaneous optical radiation from a gamma-ray burst. *Nature*, 398:400–402, 1999.

[2] G. Björnsson, E. H. Gudmundsson, and G. Jóhannesson. Energy Injection

Episodes in Gamma-Ray Bursts: The Light Curves and Polarization Properties of GRB 021004. *ApJL*, 615:L77–L80, Nov. 2004. doi: 10.1086/426477.

[3] A. Blustin, D. Band, S. Barthelmy, P. Boyd, M. Capalbi, S. T. Holland, F. E. Marshall, K. O. Mason, M. Perri, T. Poole, P. Roming, S. Rosen, P. Schady, M. Still, B. Zhang, L. Angelini, L. Barbier, A. Beardmore, A. Breeveld, D. N. Burrows, J. R. Cummings, J. Canizzo, S. Campana, M. M. Chester, G. Chincarini, L. R. Cominsky, A. Cucchiara, M. de Pasquale, E. E. Fenimore, N. Gehrels, P. Giommi, M. Goad, C. Gronwall, D. Grupe, J. E. Hill, D. Hinshaw, S. Hunsberger, K. C. Hurley, M. Ivanushkina, J. A. Kennea, H. A. Krimm, P. Kumar, W. Landsman, V. La Parola, C. B. Markwardt, K. McGowan, P. Mészáros, T. Mineo, A. Moretti, A. Morgan, J. Nousek, P. T. O'Brien, J. P. Osborne, K. Page, M. J. Page, D. M. Palmer, A. M. Parsons, J. Rhoads, P. Romano, T. Sakamoto, G. Sato, G. Tagliaferri, J. Tueller, A. A. Wells, and N. E. White. Swift Panchromatic Observations of the Bright Gamma-Ray Burst GRB 050525a. *ApJ*, 637:901–913, Feb. 2006. doi: 10.1086/498425.

[4] D. N. Burrows, J. E. Hill, J. A. Nousek, J. A. Kennea, A. Wells, J. P. Osborne, A. F. Abbey, A. Beardmore, K. Mukerjee, A. D. T. Short, G. Chincarini, S. Campana, O. Citterio, A. Moretti, C. Pagani, G. Tagliaferri, P. Giommi, M. Capalbi, F. Tamburelli, L. Angelini, G. Cusumano, H. W. Bräuninger, W. Burkert, and G. D. Hartner. The Swift X-Ray Telescope. *Space Science Reviews*, 120:165–195, Oct. 2005. doi: 10.1007/s11214-005-5097-2.

[5] S. Campana, S. Barthelmy, N. Gehrels, C. Gronwall, H. Krimm, C. Markwardt, K. Page, D. Palmer, and M. Perri. GRB 060117: Swift-BAT detection of a bright burst. *GCN 4533*, 2006.

[6] J. Cummings, L. Barbier, S. Barthelmy, E. Fenimore, N. Gehrels, K. Gendreau, D. Hullinger, H. Krimm, C. Markwardt, P. Meszaros, J. Norris, D. Palmer, A. Parsons, T. Sakamoto, G. Sato, and J. Tueller. GRB 060117: Refined analysis of the Swift-BAT burst. *GCN 4538*, 2006.

[7] A. de Ugarte Postigo, M. Jelínek, J. Gorosabel, S. McBreen, C. García-Dabó, T. Mateo Sanguino, M. D., and A. Castro-Tirado. Jibaro: Un conjunto de utilidades para la reducción y análisis automatizado de imágenes. In A. Castro-Tirado, B. de la Morena, and J. Torres, editors, *Astrofísica Robótica en España*, pages 35–50, Madrid, 2005.

[8] S. Golenetskii, R. Aptekar, E. Mazets, V. Pal'Shin, D. Frederiks, and T. Cline. Konus-Wind observation of GRB 060117. *GCN 4542*, 2006.

[9] C. Guidorzi, A. Monfardini, A. Gomboc, C. G. Mundell, I. A. Steele, D. Carter, M. F. Bode, R. J. Smith, C. J. Mottram, M. J. Burgdorf, N. R. Tanvir, N. Masetti, and E. Pian. The Early Multicolor Afterglow of GRB 050502a: Possible Evidence for a Uniform Medium with Density Clumps. *ApJL*, 630:L121–L124, Sept. 2005. doi: 10.1086/491655.

[10] M. Jelínek, P. Kubánek, M. Prouza, M. Nekola, and R. Hudec. GRB 060117: FRAM refined analysis. *GCN 4536*, 2006.

[11] P. Kubánek, M. Jelínek, M. Nekola, M. Topinka, J. Štrobl, R. Hudec, T. D. J. Mateo Sanguino, A. de Ugarte Postigo, and A. J. Castro-Tirado. RTS2 – Remote Telescope System, 2nd Version. In *AIP Conf. Proc. 727: Gamma-Ray Bursts: 30 Years of Discovery*, Sept. 2004.

[12] P. Kubánek, M. Jelínek, M. Prouza, M. Nekola, and R. Hudec. GRB 060117: FRAM optical afterglow candidate. *GCN 4535*, 2006.

[13] D. Lazzati, E. Rossi, S. Covino, G. Ghisellini, and D. Malesani. The afterglow of GRB 021004: Surfing on density waves. *A&Ap*, 396:L5–L9, Dec. 2002. doi: 10.1051/0004-6361:20021618.

[14] W. Li, A. V. Filippenko, R. Chornock, and S. Jha. The Early Light Curve of the Optical Afterglow of GRB 021211. *ApJL*, 586:L9–L12, Mar. 2003. doi: 10.1086/374684.

[15] D. B. A. Monet, B. Canzian, C. Dahn, H. Guetter, H. Harris, A. Henden, S. Levine, C. Luginbuhl, A. K. B. Monet, A. Rhodes, B. Riepe, S. Sell, R. Stone, F. Vrba, and R. Walker. The USNO-A2.0 Catalogue (Monet+ 1998). *VizieR Online Data Catalog*, 1252:0–+, Oct. 1998.

[16] M. Nysewander, A. LaCluyze, D. Reichart, J. Crain, A. Foster, and K. Ivarson. GRB 060117: PROMPT Observations. *GCN 4548*, 2006.

[17] A. Pelangeon and J. L. Atteia. GRB 060117: pseudo-z from spectral parameters of the prompt emission. *GCN 4544*, 2006.

[18] Pierre Auger Collaboration. The Pierre Auger Observatory progress and first reults. In *Proceedings of the 29th International Cosmic Ray Conference, Pune, India*, Aug. 2005.

[19] E. Rykoff, V. Mangano, S. Yost, R. Sari, F. Aharonian, C. W. Akerlof, M. C. B. Ashley, S. D. Barthelmy, D. N. Burrows, N. Gehrels, E. Göğüş, T. Güver, D. Horns, Ü. Kızılǒlu, H. A. Krimm, T. A. McKay, M. Özel, A. Phillips, R. M. Quimby, G. Rowell, W. Rujopakarn, B. E. Schaefer, D. A. Smith, H. F. Swan, W. T. Vestrand, J. C. Wheeler, J. Wren, and F. Yuan. The Anomalous Early Afterglow of GRB 050801. *ApJL*, 638:L5–L8, Feb. 2006. doi: 10.1086/501007.

[20] D. Schlegel, D. Finkbeiner, and M. Davis. Maps of Dust Infrared Emission for Use in Estimation of Reddening and Cosmic Microwave Background Radiation Foregrounds. *ApJ*, 500:525–+, June 1998. doi: 10.1086/305772.

[21] B. Schmidt, M. Wieringa, D. A. Frail, and A. Soderberg. GRB060117 - ATCA 3/6cm radio limits. *GCN 4546*, 2006.

[22] L. Shao and Z. G. Dai. A Reverse-Shock Model for the Early Afterglow of GRB 050525A. *ApJ*, 633:1027–1030, Nov. 2005. doi: 10.1086/466523.

[23] R. Shen, P. Kumar, and E. Robinson. No Universality for Electron's Power-Law Index (p) in Gamma-Ray Bursts and Other Relativistic Sources. `astro-ph/0512489`, page 1, June 2005.

[24] V. Šimon, R. Hudec, N. Masetti, and G. Pizzichini. Study of the colors of GRBs and their host galaxies. In *ESA SP-459: Exploring the Gamma-Ray Universe*, pages 441–444, Sept. 2001.

[25] N. Tanvir. GRB 060117: nearby galaxy. *GCN 4534*, 2006.

[26] Y. Terada, K. Yamaoka, S. Sugita, M. Ohno, T. Takahashi, Y. Fukazawa, K. Abe, Y. Endo, S. Hong, K. Onda, M. Tashiro, G. Sato, K. Nakazawa, T. Takahashi, R. Miyawaki, M. Kokubun, and K. Makishima. GRB 060117: Suzaku WAM observation of the prompt emission. *GCN 4573*, 2006.

[27] B. Zhang, S. Kobayashi, and P. Mészáros. Gamma-Ray Burst Early Optical Afterglows: Implications for the Initial Lorentz Factor and the Central Engine. *ApJ*, 595:950–954, Oct. 2003. doi: 10.1086/377363.

II. GRB 051028: an intrinsically faint GRB at high redshift?

The question whether a significant fraction of gamma ray bursts (GRBs) are intrinsically faint or true dark events remains unsolved [see 9, 5, and references therein]. For instance, GRB 000418 was detected in the near-IR [16] and it is one of the reddest (R-K = 4) together with GRB 980329 [28], GRB 030115 [17] and the recent GRB 050915A [3]. In most cases, it has been suggested that the cause of the reddening was dust extinction in the host galaxy. On the other hand, GRB 021211 was found to be very dim at 24 hours, as a scaled-down version of GRB 990123 [21].[2)]

With the launch of *Swift* in Nov 2004, which has the ability to follow-up the events detected by the GRB detector onboard (BAT) or by other satellites like *HETE-2* and

[2)] Based on observations taken with the 1.34m Tautenburg telescope in Germany, with the 2.0 m Himalayan Chandra Telescope in India and with the 4.2 m William Herschel telescope at the Spanish Observatorio del Roque de los Muchachos in Canary Islands.

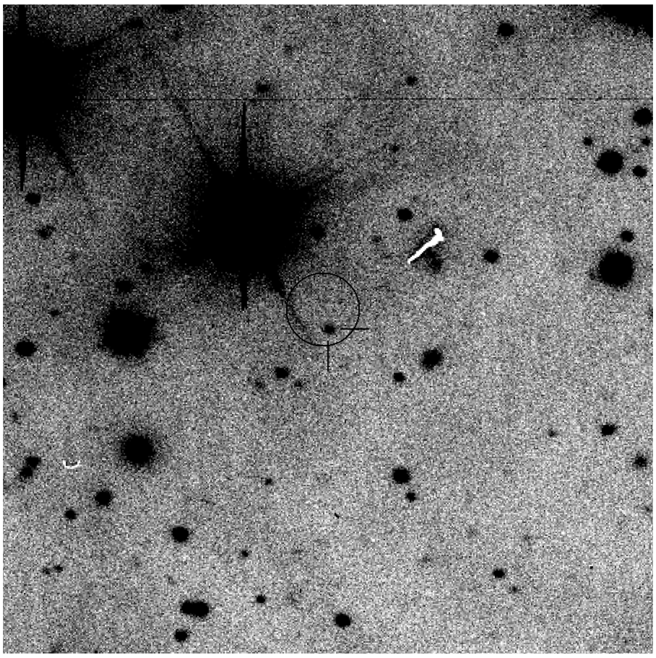

Figure 4: The deep *R* band image of the GRB 051028 field taken at the 4.2WHT on 28 Oct 2005. The optical afterglow within the $3\farcs8$ *Swift*/XRT error box (circle) is depicted. The field is $2'.5 \times 1'.9$ with North up and East to the left.

Table 2: Journal of optical observations of the GRB 051028 field.

Date of 2005 UT (mid exposure)	Telescope/ Instrument	Filter	Exposure Time (seconds)	Magnitude
Oct 28, 16:18	2.0 HCT (HFOSC)	R_c	300	20.63±0.04
Oct 28, 16:32	2.0 HCT (HFOSC)	R_c	300	20.72±0.05
Oct 28, 16:47	2.0 HCT (HFOSC)	R_c	300	21.14±0.07
Oct 28, 17:03	2.0 HCT (HFOSC)	R_c	300	21.27±0.07
Oct 28, 17:43	1.34 Taut (CCD)	R_c	1 080	21.23±0.13
Oct 28, 17:47	2.0 HCT (HFOSC)	R_c	300	21.17±0.08
Oct 28, 21:42	4.2 WHT (PFC)	R	300	21.97±0.05
Oct 29, 05:47	4.2 WHT (PFC)	R	120	22.8±0.3
Oct 29, 20:15	4.2 WHT (PFC)	R	720	>23.7
Oct 31, 22:14	4.2 WHT (PFC)	R	2 700	>25.1
Oct 28, 16:25	2.0 HCT (HFOSC)	I_c	300	19.79±0.11
Oct 28, 16:39	2.0 HCT (HFOSC)	I_c	300	19.94±0.06
Oct 28, 16:55	2.0 HCT (HFOSC)	I_c	300	20.29±0.09
Oct 28, 17:09	1.34 Taut (CCD)	I_c	1 080	20.5 ± 0.3
Oct 28, 17:10	2.0 HCT (HFOSC)	I_c	300	20.38±0.08
Oct 28, 17:55	2.0 HCT (HFOSC)	I_c	300	20.35±0.09
Oct 28, 19:12	1.34 Taut (CCD)	I_c	1 800	20.67±0.23
Oct 28, 20:33	1.34 Taut (CCD)	I_c	3 600	20.75±0.13
Oct 28, 22:50	1.34 Taut (CCD)	I_c	5 400	21.16±0.16
Oct 28, 18:28	1.34 Taut (CCD)	V	1 080	22.08±0.20

INTEGRAL, it is possible to zoom in on this population of optically faint events in order to disentangle their nature.

GRB 051028 was one of such event. It was discovered by *HETE-2* on 28 Oct 2005, lying (90% confidence) on a 33′× 18′error box centred at coordinates: RA (J2000) = $01^h48^m38\overset{s}{.}6$ Dec (J2000) = +47°48′30.″0 [13]. The burst started at T_0 = 13:36:01.47 UT and a value of T_{90} = 16 s is derived, putting it in the "long-duration" class of GRBs. It had a fluence of 6×10^{-7} erg cm^{-2} in the 2-30 keV range and 6×10^{-6} erg cm^{-2} in the 30-400 keV range [13]. This event was also detected by *Konus*/WIND in the 20 keV - 2 MeV range, with a duration of ≈ 12 s, a fluence of $(6.78^{+0.61}_{-1.08}) \times 10^{-6}$ erg cm^{-2} in the 20 keV - 2 MeV range and a peak energy $E_p = 298^{+73}_{-50}$ keV [11]. *Swift*/XRT started to observe the field ~ 7.1 hours after the event and detected the X-ray afterglow 5.2′ away from the center of the initial *HETE − 2* error box [27].

We report here results of multi-wavelength observations in optical and X-ray waveband and discuss the reasons for the apparent optical faintness of GRB 051028 in comparison with other bursts.

2.1 X-ray observations

We availed ourselves of the public X-ray observations from *Swift*/XRT which consists of four observations starting ~ 7.1, 120, 150 and 230 hours after the event respectively. The detection in the first observation is significant (signal-to-noise ratio S/N~13.5), but in later observations the X-ray afterglow is weaker and it is detected with a signal-to-noise of 3.3, 2.9 and 2.7.

The XRT data is in photon counting mode and were reduced using the standard

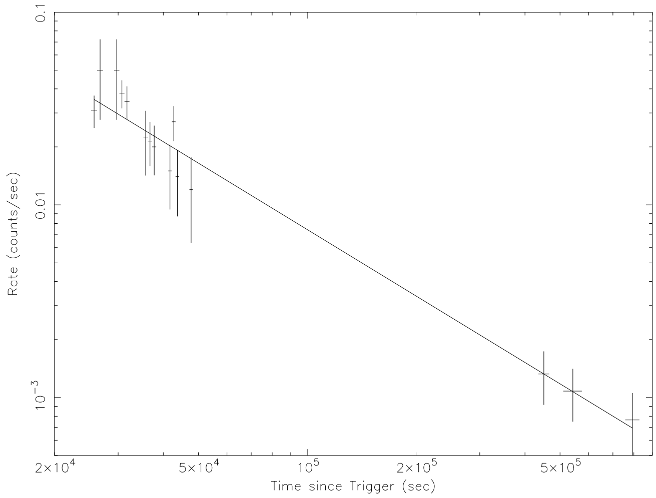

Figure 5: The X-ray lightcurve obtained by *Swift*/XRT starting 7.1 hours after the event onset and continuing up to 10 days later. The data are fit by a power-law decline exponent $\alpha_X = -1.1^{+0.1}_{-0.2}$.

pipeline for XRT data using *Swift* software version 2.2[3] and using the most recent calibration files. The data were analysed with the XSPEC version 11.3 [1] . Source and background regions were extracted using a circular aperture. Spectra were selected to have at least 20 counts/bin.

2.2 Optical observations

Target of Opportunity (ToO) observations in the optical were triggered starting 2.7 hours after the event at the 2.0 m Himalayan Chandra Telescope (HCT) at Indian Astronomical Observatory (HCO). 10′× 10′ frames were taken in imaging mode with the Himalaya Faint Object Spectrograph (HFOSC), covering only the central part of the large (33′× 18′) *HETE-2* error box. Additional observations were conducted at the 1.34m Schmidt telescope in Tautenburg (providing a 42′× 42′ FOV and thus covering the large error box) and at the 4.2 m William Herschel Telescope (WHT + Prime Focus Camera) at Observatorio del Roque de los Muchachos in La Palma (Spain). A mosaic of 2 images (15′× 15′ FOV) were taken in order to cover the entire *HETE-2* error box. Subsequently, follow-up observations were taken on the following days at the 4.2 m WHT. Table 2 displays the observing log. The optical field was calibrated using the calibration files provided by Henden [12].

2.3 The X-ray afterglow

The X-ray data confirm the presence of a decaying X-ray source in the fraction (70 %) of the *HETE-2* error box covered by the *Swift*/XRT, as previously reported by Racusin et al. (2005). The X-ray position is RA(J2000) = $01^h48^m15\overset{s}{.}1$, Dec(J2000) = +47°45′12.″9 (l^{II} = 132°.72, b^{II} = -14°.03), with an estimated uncertainty of 3.″8 [19, 90% containment].

[3] http://swift.gsfc.nasa.gov/docs/software/lheasoft/ /download.html

The X-ray light curve in the energy range 0.3 to 10 keV is shown in Fig. 1. The early X-ray light curve (2×10^4 to 5×10^4 s) can be fit by a power-law decay $F_X \propto t^{\alpha_X}$ with exponent $\alpha_X = -1.43\pm0.60$ with a χ^2/d.o.f = 9.3/10. The data were also fit including the late time data up to 10 days (~8.6×10^5 s) and resulted in a exponent $\alpha_X = -1.1^{+0.15}_{-0.2}$ with χ^2/d.o.f = 10.7/13) compatible with the power-law index obtained considering only the early observations. The value of α_X is dominated by the late time data and a break or flattening of the light curve at intervening times is possible and cannot be excluded by the observations.

A spectrum was extracted for the first observation starting at 7.1 hours consisting of 5 *Swift* orbits. The X-ray spectrum was fit by an absorbed power-law with photon index $\Gamma=2.3^{+0.30}_{-0.25}$ with a column density $N_H = 0.40^{+0.30}_{-0.25} \times 10^{22}$ cm^{-2} (with χ^2/d.o.f = 9.1/9) (Fig. 2). The galactic column density, $N_{H,GAL}$, was estimated to be 1.2×10^{21}cm^{-2} using the weighted average of 6 points within 1°of the source location [4] [7]. The values used to estimate $N_{H,GAL}$ range from 1.01×10^{21}cm^{-2} to 1.33×10^{21}cm^{-2}. The fitted spectrum is compatible at 90% confidence level with Galactic absorption of 1.2×10^{21}cm^{-2} (Fig. 3). A power-law index of $\Gamma = 1.7 \pm 0.2$ (χ^2/d.o.f = 12.8/10) (i.e. a spectral X-ray index $\beta_X = -0.7 \pm 0.2$ with $F(\nu) \propto \nu^\beta$) is obtained if only Galactic absorption $N_{H,GAL}$ of 1.2×10^{21}cm^{-2} is considered in agreement with Page et al. (2005). Alternatively, if we assume that all of the extra absorption originates in the host galaxy and freeze the $N_{H,GAL}$ at 1.2×10^{21}cm^{-2} then the intrinsic absorption in the host at the pseudo-z (see below) of z=3.7 is $N_{H,z=3.7}$ of $12.2^{+18.5}_{-12.1}\times10^{22}$cm^{-2}.

2.4 The optical afterglow

The optical counterpart was discovered on our *R*-band images taken at the 4.2m WHT telescope starting 7.5 hours after the onset of the gamma-ray event. A faint $R = 21.9$ object was detected inside the *Swift*/XRT error circle [15, 22]. Astrometry against USNO-B yielded the coordinates: RA(J2000) = $01^h48^m15\overset{s}{.}00$, Dec(J2000) = $+47°45'09\overset{''}{.}4$, with $0\overset{''}{.}2$ uncertainty (1σ, see Fig. 4).

[4] http://heasarc.gsfc.nasa.gov/cgi-bin/Tools/w3nh/w3nh.pl

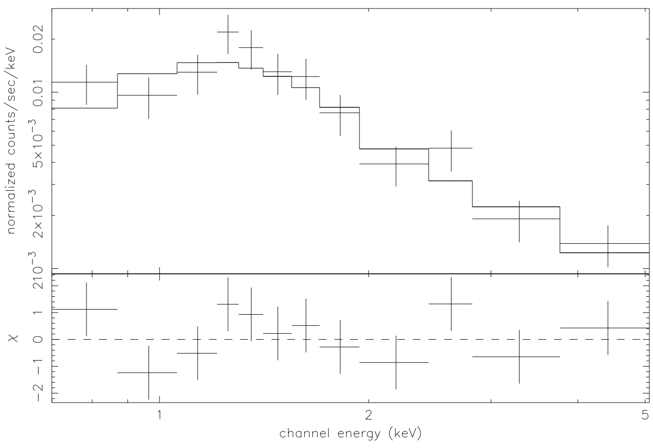

Figure 6: The X-ray spectrum obtained by *Swift*/XRT for the time interval T_0 + 7.1 hours to T_0 + 13.2 hours. The data can be fitted by a power-law with photon index $\Gamma = 2.3^{+0.30}_{-0.25}$.

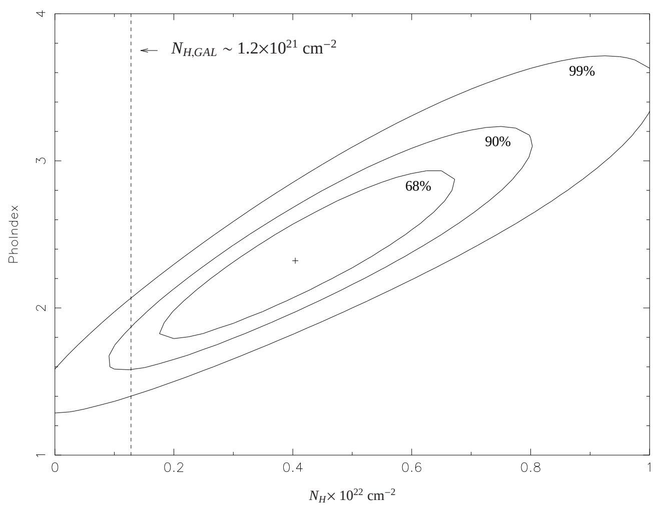

Figure 7: Contour plot of column density versus photon index for the absorbed power law model shown in Figure 2. The dashed line shows the estimated Galactic column density value 1.2×10^{21} cm^{-2} and the contours denote 68%, 90% and 99% confidence levels respectively. The spectrum is compatible (90% confidence) with Galactic absorption.

With E(B-V) = 0.21 in the line of sight [30], $A_V = 0.71$ is derived (which translates into $A_V = 0.6$ if the correction factor proposed by Dutra et al. [8] is taken into account). A value of $A_V = 0.7$ is obtained using the fit from Predehl and Schmitt [26] for the Galactic H column. We choose $A_V \sim 0.7$ for the rest of this paper, which implies A_R = 0.53 and A_I = 0.37.

From the analysis of the full *VRI* dataset available obtained at Hanle, Tautenburg and La Palma, we have obtained the optical afterglow lightcurve plotted in Fig. 5. The data between T_0 + 4 hours and T_0 + 15 hours can be fitted by a shallow power-law decline with decay index $\alpha_{opt} = -0.9 \pm 0.1$. The upper limits obtained at 1.5 and 3.5 day (>23.7 and >25.1 respectively) may suggest the existence of a break in the lightcurve after ~ 1 day.

The data prior to 4 hours (i.e. in the range T_0 + 2.7 hours and T_0 + 4 hours) show a bumpy behaviour very similar to the one seen in other events like GRB 021004 [6], GRB 030329 (Guziy et al. 2006 and references therein) and GRB 050730 [23]. In fact, the similarity with GRB 050730 is very remarkable, if GRB 051028 is shifted up by 3 magnitudes (Fig. 6). There is evidence for at least two of such bumps taking place, superimposed on the power-law decline. This could be explained in the framework of multiple energy injection episodes [2]. GRB 050730 is an optically bright afterglow [see Fig. 12 of 18] whereas GRB 051028 seems an optically faint event if at redshift $z \sim$ 3-4. Unfortunately there is no X-ray data available at this epoch to allow a more complete modelling being carried out.

2.5 A high redshift event

We have extrapolated the optical and X-ray fluxes of the GRB 051028 afterglow to T_0 + 11 hours and derived a value of $\beta_{opt-X} = -0.55 \pm 0.05$. Thus GRB 051028 is located in the "gray" or "potentially dark" GRB locus on the dark GRB diagram by Jakobsson et al. [14]. How can the optical faintness of GRB 051028 be explained ?

Although the redshift of this event could not be properly measured due to its faintness at the time of the discovery, we are able to constrain it on the basis of the *VRI*-band data presented in this paper. Using the magnitudes derived here and correcting them for the Galactic extinction in the line of sight, we determine a spectral optical index $\beta_{opt} = -2.1 \pm 0.4$. In the simplest fireball models [29], $F_\nu \propto \nu^\beta$ with $\beta = -p/2$ for $\nu > \nu_c$ and $\beta = -(p\text{-}1)/2$ for $\nu < \nu_c$. Thus, for a typical range of p values in the range $1.5 < p < 3$ [31], β_{opt} should be in the range $-1.5 < \beta_{opt} < -0.25$. In fact, the GRB 051028 X-ray data before T_0 + 0.5 day are well fitted by a jet model with $p = 2.4$ in the slow cooling case, moving through the ISM (with ρ = constant) prior to the jet break time and with a cooling frequency ν_c still above the X-rays. A value of $\Gamma = 1.7$ is favoured (as $\Gamma = 2.3$ is giving high, unrealistic values of p) and thus we can consider that all the absorption is Galactic in origin (and ruling out dust along the line of sight in the host galaxy). The X-ray data (both values of Γ) are also eventually fitted for a value of p = 2.1 if ν_c would have already crossed the X-ray band at that time (0.5 d), as it seems to be derived from a sample of events studied by *BeppoSAX* [25], but this is unlikely in the light of the recent *Swift*/XRT results for a sample of (presumably higher-z) events [20]. In any of the above mentioned cases, the observed value of α_{opt} can be reproduced and therefore β_{opt} should be ~ -0.7. What is the reason for the discrepancy in the observed and expected values of β_{opt} ?

Fig. 7 shows the derived β_{opt} when using *only VRI* magnitudes for a sample of bursts in the range $3.3 < z < 4.5$. As can be seen the derived values are in the range of the one found for GRB 051028, well above the β_{opt} = 1.5 value mentioned previously.

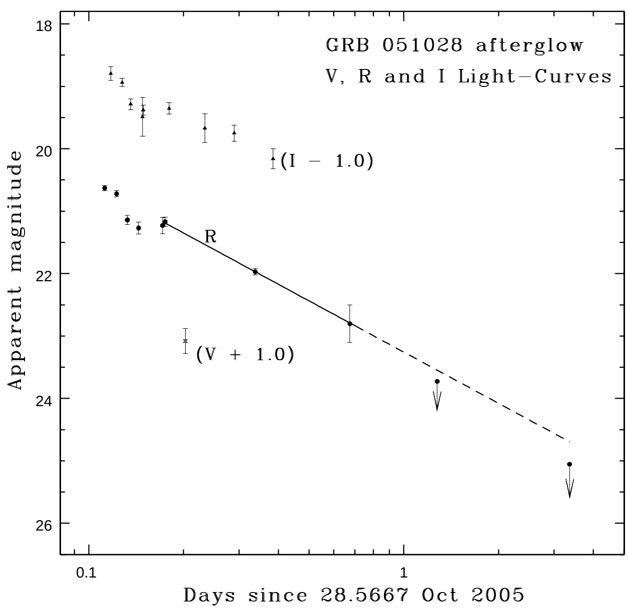

Figure 8: The *R* and *I*-band lightcurves (including the *V*-band single detection) obtained at Hanle (HCT), Tautenburg and La Palma (WHT) starting 2.7 hours after the event onset and continuing up to 3.5 days later. The data after 4.0 hours are fit by a power-law decline exponent $\alpha_{opt} = -0.9 \pm 0.1$.

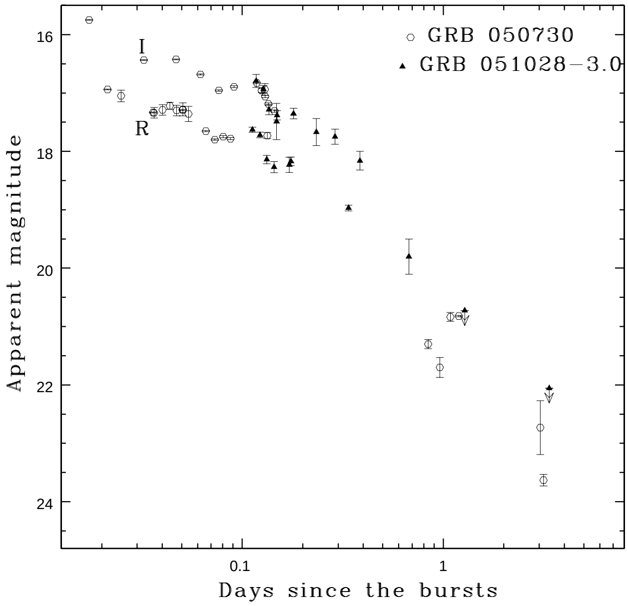

Figure 9: The GRB 051028 *R* and *I*-band light curves shifted by ∼ 3 mag in order to match the GRB 050730 *R*-band lightcurve (from Pandey et al. 2006). No shift in the T-T_0 values has been performed. These combined data strengthen the evidence of a "bumpy" behaviour of the GRB 051028 afterglow.

This is naturally explained by the fact that at $z \sim 3.2$ and ∼4.0, the Lyman-α break begins affecting the *V* and *R* passbands respectively. Therefore, one *natural* explanation for the β_{opt} value found for GRB 051028 is that it also arose at a $z \approx 3{-}4$, a value to be compared with that of GRB 050730 ($z = 3.967$), a burst which has a suprisingly similar optical afterglow lightcurve, as we have shown in Section 3.2. This $z \approx 3{-}4$ value is in fact in agreement with the pseudo-$z = 3.7 \pm 1.8$ derived for this burst using the recent pseudo-*z* estimator developed by Pélangeon et al. [24] on the basis of the observed peak energy and the bolometric luminosity in the 15 sec long interval containing the highest fluence. This would be in agreement with the fact that no host galaxy is detected down to $R = 25.1$. This high-redshift is also supported by the late break time, as typical afterglows undergo a jet break episode before T_0 + 1 day in the rest frame [31]. In fact, the Ghirlanda et al. [10] $E_p - E_\gamma$ relation is satisfied for GRB 051028 when considering the pseudo-$z = 3.7$.

The fact that the afterglow of GRB 051028 is not unusual in the *Swift*/XRT sample may indicate that the density of the surrounding medium where the progenitor has taken place should be closer to the the typical value of ≈ 1 cm^{-3} derived for several long-duration GRBs. So a low density environment is not the reason for its faintness at optical wavelengths. It could be that GRB 051028 could be an underluminous GRB similar to GRB 980613, GRB 011121 and GRB 021211 (see Nardini et al. and references therein), in contrast to GRB 050730.

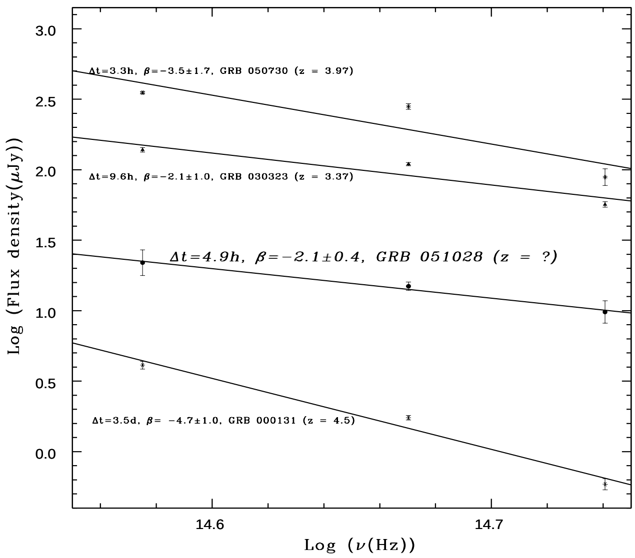

Figure 10: The β_{opt} spectral indexes obtained for GRB optical afterglows in the redshift range $3 < z < 4.5$ based solely on the *VRI* data. The β_{opt} value derived for GRB 051028 is in the range of those derived for this high-z sample and therefore supports that GRB 051028 also arose at a z = 3-4.

2.6 Conclusions

We have presented multiwavelength observations of the long duration GRB 051028 detected by *HETE-2* between 2.7 hours and ~ 10 days after the event. The X-ray afterglow of GRB 051028 can be compared to other GRB afterglows in the sense that its flux at 11 hours is typical, i.e., one can assume that the burst has occurred on a classical n ~ 1 cm^{-3} environment. The optical afterglow, on the other hand, is dim at a similar epoch (and comparable for instance to GRB 030227, citetct03. We also noticed the remarkable similarity to the optical afterglow of GRB 050730, a burst lasting ~ 10 times longer with comparable gamma-ray fluence[5] at z = 3.967 (see Pandey et al. 2006 and references therein). This indicates that the faintness of the optical emission is not due to a low-density environment as in the case of some short GRBs, such as GRB 050509b [4]. Instead, we propose that GRB 051028 occurred in a faint galaxy (with R >25.1) at a high redshift consistent with the pseudo-z = 3.7 ± 1.8.

Thanks to the extraordinary repointing capabilities of *Swift*, the accurate localisations for future events and the corresponding multiwavelength follow-up will shed more light on the origin of this faint optical afterglow population.

References

[1] K. A. Arnaud. XSPEC: The First Ten Years. In G. H. Jacoby and J. Barnes, editors, *Astronomical Data Analysis Software and Systems V*, volume 101 of *Astronomical Society of the Pacific Conference Series*, page 17, 1996.

[5] The scarcity of the available X-ray data for GRB 051028 does not allow to make a straigth comparison with respect to the GRB 050730 X-ray afterglow.

[2] G. Björnsson, E. H. Gudmundsson, and G. Jóhannesson. Energy Injection Episodes in Gamma-Ray Bursts: The Light Curves and Polarization Properties of GRB 021004. *ApJL*, 615:L77–L80, Nov. 2004. doi: 10.1086/426477.

[3] J. S. Bloom and K. Alatalo. GRB 050915: IR observations. *GRB Coordinates Network*, 3984:1, 2005.

[4] A. J. Castro-Tirado, A. de Ugarte Postigo, J. Gorosabel, T. Fathkullin, V. Sokolov, M. Bremer, I. Márquez, A. J. Marín, S. Guziy, M. Jelínek, P. Kubánek, R. Hudec, S. Vitek, T. J. Mateo Sanguino, A. Eigenbrod, M. D. Pérez-Ramírez, A. Sota, J. Masegosa, F. Prada, and M. Moles. <ASTROBJ>GRB 050509b</ASTROBJ>: the elusive optical/nIR/mm afterglow of a short-duration GRB. *A&Ap*, 439:L15–L18, Aug. 2005. doi: 10.1051/0004-6361:200500147.

[5] A. J. Castro-Tirado, M. Bremer, S. McBreen, J. Gorosabel, S. Guziy, T. A. Fakthullin, V. V. Sokolov, R. M. González Delgado, G. Bihain, S. B. Pandey, M. Jelínek, A. de Ugarte Postigo, K. Misra, R. Sagar, P. Bama, A. P. Kamble, G. C. Anupama, J. Licandro, D. Pérez-Ramírez, D. Bhattacharya, F. J. Aceituno, and R. Neri. The dark nature of <ASTROBJ>GRB 051022</ASTROBJ> and its host galaxy. *A&Ap*, 475:101–107, Nov. 2007. doi: 10.1051/0004-6361:20066748.

[6] A. de Ugarte Postigo, A. J. Castro-Tirado, J. Gorosabel, G. Jóhannesson, G. Björnsson, E. H. Gudmundsson, M. Bremer, S. Pak, N. Tanvir, J. M. Castro Cerón, S. Guzyi, M. Jelínek, S. Klose, D. Pérez-Ramírez, J. Aceituno, A. Campo Bagatín, S. Covino, N. Cardiel, T. Fathkullin, A. A. Henden, S. Huferath, Y. Kurata, D. Malesani, F. Mannucci, P. Ruiz-Lapuente, V. Sokolov, U. Thiele, L. Wisotzki, L. A. Antonelli, C. Bartolini, A. Boattini, A. Guarnieri, A. Piccioni, G. Pizzichini, M. del Principe, A. di Paola, D. Fugazza, G. Ghisellini, L. Hunt, T. Konstantinova, N. Masetti, E. Palazzi, E. Pian, M. Stefanon, V. Testa, and P. J. Tristram. GRB 021004 modelled by multiple energy injections. *A&Ap*, 443: 841–849, Dec. 2005. doi: 10.1051/0004-6361:20052898.

[7] J. M. Dickey and F. J. Lockman. H I in the Galaxy. *ARAA*, 28:215–261, 1990. doi: 10.1146/annurev.aa.28.090190.001243.

[8] C. M. Dutra, A. V. Ahumada, J. J. Clariá, E. Bica, and B. Barbuy. On the calibration of the COBE/IRAS dust emission reddening maps. *A&Ap*, 408:287–295, Sept. 2003. doi: 10.1051/0004-6361:20030980.

[9] P. Filliatre, P. D'Avanzo, S. Covino, D. Malesani, G. Tagliaferri, S. McGlynn, L. Moran, P. Goldoni, S. Campana, G. Chincarini, L. Stella, M. Della Valle, N. Gehrels, S. McBreen, L. Hanlon, B. McBreen, J. A. Nousek, and R. Perna. Out of the darkness: the infrared afterglow of the INTEGRAL burst <ASTROBJ>GRB 040422</ASTROBJ> observed with the VLT. *A&Ap*, 438:793–801, Aug. 2005. doi: 10.1051/0004-6361:20042609.

[10] G. Ghirlanda, G. Ghisellini, and D. Lazzati. The Collimation-corrected Gamma-Ray Burst Energies Correlate with the Peak Energy of Their νF_ν Spectrum. *ApJ*, 616:331–338, Nov. 2004. doi: 10.1086/424913.

[11] S. Golenetskii, R. Aptekar, E. Mazets, V. Pal'Shin, D. Frederiks, and T. Cline. Konus-wind observation of GRB 051028. *GRB Coordinates Network*, 4183:1, 2005.

[12] A. Henden. Recent GRB UBVRcIc field photometry. *GRB Coordinates Network*, 4184:1–+, 2005.

[13] K. Hurley, G. Ricker, J.-L. Atteia, N. Kawai, D. Lamb, S. Woosley, M. Arimoto, T. Donaghy, E. Fenimore, M. Galassi, C. Graziani, N. Ishikawa, A. Kobayashi, J. Kotoku, M. Maetou, M. Matsuoka, Y. Nakagawa, T. Sakamoto, R. Sato, T. Shimokawabe, Y. Shirasaki, S. Sugita, M. Suzuki, T. Tamagawa, K. Tanaka, A. Yoshida, N. Butler, G. Crew, J. Doty, G. Prigozhin, R. Vanderspek, J. Villasenor, J. G. Jernigan, A. Levine, G. Azzibrouck, J. Braga, R. Manchanda, G. Pizzichini, M. Boer, J.-F. Olive, and J.-P. Dezalay. GRB 051028 (=H3951): a GRB localized by HETE. *GRB Coordinates Network*, 4172:1, 2005.

[14] P. Jakobsson, J. Hjorth, J. P. U. Fynbo, D. Watson, K. Pedersen, G. Björnsson, and J. Gorosabel. Swift Identification of Dark Gamma-Ray Bursts. *ApJL*, 617: L21–L24, Dec. 2004. doi: 10.1086/427089.

[15] M. Jelinek, S. B. Pandey, S. S. Guziy, J. Gorosabel, A. de Ugarte Postigo, S. Vitek, and J. T. A. de Jong. GRB051028: WHT optical candidate. *GRB Coordinates Network*, 4175:1, 2005.

[16] S. Klose, B. Stecklum, N. Masetti, E. Pian, E. Palazzi, A. A. Henden, D. H. Hartmann, O. Fischer, J. Gorosabel, C. Sánchez-Fernández, D. Butler, T. Ott, S. Hippler, M. Kasper, R. Weiss, A. Castro-Tirado, J. Greiner, C. Bartolini, A. Guarnieri, A. Piccioni, S. Benetti, F. Ghinassi, A. Magazzú, K. Hurley, T. Cline, J. Trombka, T. McClanahan, R. Starr, J. Goldsten, R. Gold, E. Mazets, S. Golenetskii, K. Noeske, P. Papaderos, P. M. Vreeswijk, N. Tanvir, A. Oscoz, J. A. Muñoz, and J. M. Castro Cerón. The Very Red Afterglow of GRB 000418: Further Evidence for Dust Extinction in a Gamma-Ray Burst Host Galaxy. *ApJ*, 545:271–276, Dec. 2000. doi: 10.1086/317816.

[17] A. Levan, A. Fruchter, J. Rhoads, B. Mobasher, N. Tanvir, J. Gorosabel, E. Rol, C. Kouveliotou, I. Dell'Antonio, M. Merrill, E. Bergeron, J. M. Castro Cerón, N. Masetti, P. Vreeswijk, A. Antonelli, D. Bersier, A. Castro-Tirado, J. Fynbo, P. Garnavich, S. Holland, J. Hjorth, P. Nugent, E. Pian, A. Smette, B. Thomsen, S. E. Thorsett, and R. Wijers. Infrared and Optical Observations of GRB 030115 and its Extremely Red Host Galaxy: Implications for Dark Bursts. *ApJ*, 647: 471–482, Aug. 2006. doi: 10.1086/503595.

[18] M. Nardini, G. Ghisellini, G. Ghirlanda, F. Tavecchio, C. Firmani, and D. Lazzati. Clustering of the optical-afterglow luminosities of long gamma-ray bursts. *A&Ap*, 451:821–833, June 2006. doi: 10.1051/0004-6361:20054085.

[19] K. L. Page, M. R. Goad, D. N. Burrows, J. Racusin, S. Oates, M. Ajello, and M. Trippico. GRB051028: Swift-XRT refined analysis. *GRB Coordinates Network*, 4205:1, 2005.

[20] A. Panaitescu, P. Mészáros, D. Burrows, J. Nousek, N. Gehrels, P. O'Brien, and R. Willingale. Evidence for chromatic X-ray light-curve breaks in Swift gamma-ray burst afterglows and their theoretical implications. *MNRAS*, 369:2059–2064, July 2006. doi: 10.1111/j.1365-2966.2006.10453.x.

[21] S. B. Pandey, G. C. Anupama, R. Sagar, D. Bhattacharya, A. J. Castro-Tirado, D. K. Sahu, P. Parihar, and T. P. Prabhu. The optical afterglow of the not so dark GRB 021211. *A&Ap*, 408:L21–L24, Sept. 2003. doi: 10.1051/0004-6361:20031153.

[22] S. B. Pandey, M. Jelinek, S. S. Guziy, J. Gorosabel, A. de Ugarte Postigo, S. Vitek, and J. T. A. de Jong. GRB051028: confirmation of the afterglow. *GRB Coordinates Network*, 4176:1–+, 2005.

[23] S. B. Pandey, A. J. Castro-Tirado, S. McBreen, M. D. Pérez-Ramírez, M. Bremer, M. A. Guerrero, A. Sota, B. E. Cobb, M. Jelínek, A. de Ugarte Postigo, J. Gorosabel, S. Guziy, C. Guidorzi, C. D. Bailyn, T. Muñoz-Darias, A. Gomboc, A. Monfardini, C. G. Mundell, N. Tanvir, A. J. Levan, B. C. Bhatt, D. K. Sahu, S. Sharma, O. Bogdanov, and J. A. Combi. Multi-wavelength afterglow observations of the high redshift GRB 050730. *A&Ap*, 460:415–424, Dec. 2006. doi: 10.1051/0004-6361:20065010.

[24] A. Pélangeon, J.-L. Atteia, D. Q. Lamb, and Hete-2 Science Team. An improved redshift indicator for Gamma-Ray Bursts, based on the prompt emission. In S. S. Holt, N. Gehrels, and J. A. Nousek, editors, *Gamma-Ray Bursts in the Swift Era*, volume 836 of *American Institute of Physics Conference Series*, pages 149–152, May 2006. doi: 10.1063/1.2207877.

[25] L. Piro. Sommario (Table of Contents). *Nuovo Cimento C Geophysics Space Physics C*, 28:473–+, July 2005. doi: 10.1393/ncc/i2005-10088-2.

[26] P. Predehl and J. H. M. M. Schmitt. X-raying the interstellar medium: ROSAT observations of dust scattering halos. *A&Ap*, 293:889–905, Jan. 1995.

[27] J. Racusin, K. Page, J. Kennea, D. Morris, C. Pagani, D. Burrows, and N. Gehrels. GRB051028: swift XRT position. *GRB Coordinates Network*, 4174:1–+, 2005.

[28] D. E. Reichart, D. Q. Lamb, M. R. Metzger, J. M. Quashnock, D. M. Cole, F. J. Castander, S. Klose, J. E. Rhoads, A. S. Fruchter, A. R. Cooray, and D. E. vanden Berk. Optical and Near-infrared Observations of the Afterglow of GRB 980329 from 15 Hours to 10 Days. *ApJ*, 517:692–699, June 1999. doi: 10.1086/307210.

[29] R. Sari, T. Piran, and R. Narayan. Spectra and Light Curves of Gamma-Ray Burst Afterglows. *ApJL*, 497:L17, Apr. 1998. doi: 10.1086/311269.

[30] D. Schlegel, D. Finkbeiner, and M. Davis. Maps of Dust Infrared Emission for Use in Estimation of Reddening and Cosmic Microwave Background Radiation Foregrounds. *ApJ*, 500:525–+, June 1998. doi: 10.1086/305772.

[31] A. Zeh, S. Klose, and D. A. Kann. Gamma-Ray Burst Afterglow Light Curves in the Pre-Swift Era: A Statistical Study. *ApJ*, 637:889–900, Feb. 2006. doi: 10.1086/498442.

III. Four Years of Realtime GRB Followup by BOOTES-1B (2005-2008)

3.1 Introduction

BOOTES-1B (see also Castro-Tirado et al. 1999 [1], Castro-Tirado et al. 2004 [2]) is an independent robotic observatory with a 30 cm aperture telescope dedicated primarily to follow-up of gamma-ray burst (GRBs). Since 2003 it has used RTS2 [3] as an observing system. It is located at the atmospheric sounding station (Estación de Sondeos Atmosféricos — ESAt, INTA) of El Arenosillo in Andalucía, Spain (at lat: $37°06'16''$N, long: $06°43'\ 58''$W). A nearby, older dome (BOOTES-1A) is used for complementary wider angle instruments.

We present results of our GRB follow-up programme. In a large table, we show a 4 year long follow-up log of BOOTES-1B GRBs — all triggers available in real time which were, or should have been received and processed by the system. This selected sample of GRBs is then used to provide a basic idea of how much time is needed at the telescope to observe GRB optical afterglows.

3.2 Robotic Telescope Configuration

The telescope is built mostly from commercially available components — a Paramount ME from Software Bisque and a D=30 cm Schmidt-Cassegrain optical tube assembly from Meade. Over time, four distinct system configurations were used, including also two 8 inch S-C telescopes.

3.2.1 Original Meade — stereoscopic system

The original BOOTES project idea of a new generation of robotic telescopes was very simple, BOOTES-1B would — simultaneous with an identical setup at BOOTES-2 for parallax ability — look for optical transients in an extended area of the sky with wide field cameras. Both systems would use a commercial 12-inch Meade LX-200 "robot". The wide-field cameras were considered a primary instrument, while the ability to follow-up with a large telescope was an option. Between 1998 and 2002 the wide-field system provided simultaneous limits for several *CGRO*/BATSE and *BeppoSAX* GRBs, most notably the candidate afterglow for the short GRB 000313 [4]. The 30 cm telescope was successfully used to follow-up GRB 030329.

Although we made the original system able to observe, it kept having problems. It required an operator presence several times per week and, despite a notable effort, the fork mount's electronics had to be exchanged several times. Because of that, we decided to purchase another mount.

Figure 11: Four historic BOOTES-1B configurations.

3.2.2 The Prototype

The new incarnation of BOOTES-1B was in preparation since mid-2002, and the first prototype was put together in November 2002 in order to follow-up *INTEGRAL* bursts. The most important change was the mount to be used — the Paramount ME from Software Bisque. The system was still carrying a wide field camera, but a shift had been made in priorities — the wide field camera performed monitoring of satellite field of view and the telescope pointed when a trigger was received. The early stage was, however, plagued with technical and organizational problems which eventually delayed the first real-time real-GRB follow-up until early 2005.

The prototype carried three instruments on a large aluminium base plate: The 30 cm telescope with a field spectrograph [5] plus an SBIG-ST8 camera, the 20 cm Meade (originally BOOTES-1A) telescope with an SBIG-ST9 camera observing in a fixed V-band filter, and an unfiltered wide-field 18 mm/1:2.8 with an SBIG ST-8 CCD (43°×29°).

BOOTES-1B was operating with this setup for about a year — on June 2004 it was dismounted and sent to the Workshop in Ondřejov for a definitive solution.

3.2.3 Triple Telescope

The prototype was very heavy and from the beginning had some problems. In September 2004 BOOTES-1B finally received an upgrade — together with the 30 cm telescope, there were also two 20 cm telescopes[6] for direct imaging in different filters. The system was completely redesigned with many mechanical improvements and was built to be as light as possible to allow the mount working at its maximum slewing

[6] One of them lent personally by AJCT

Figure 12: The building of ESAt with domes of BOOTES-1A and BOOTES-1B (2002).

speed. In belief that the rapid dissemination and fast followup after the launch of *Swift* would lead into relatively frequent detections of bright optical counterparts, the 30 cm telescope was equipped with a field spectrograph and two 20 cm telescopes with fixed V&I-band filters. The limiting magnitude of all three instruments was V ~ 16 for a 60 s exposure. The wide-field cameras were moved from BOOTES-1B to BOOTES-1A.

Later, during the telescope operation it became clear that the GRB optical transients were not as bright as had been expected and so the spectrograph on the 30 cm telescope was replaced with a direct imaging CCD with R-band filter — improving the limiting magnitude but losing the spectroscopic ability.

On April 23, 2006, The ESAt building was struck by lightning during a storm, destroying a major part of BOOTES-1B electronics. It took more than a year to get BOOTES-1B definitively back online.

3.2.4 Single 30 cm telescope

During the lengthy reconstruction of BOOTES-1B, the followup strategy was reconsidered: in the interest of detecting more optical transients the filter(s) were abandoned (~2.5× or 1 magnitude gain in sensitivity). The limiting magnitude of an unfiltered 120 s exposure would be about 18.0 — effectively doubling the likelihood of getting an optical transient in comparison with the R-band imaging (cf. Fig. 14). Both 20 cm telescopes were dropped because of lack of suitable CCD cameras available for them. Since then, BOOTES-1B has only a single 30 cm telescope.

Any observations obtained after June 15, 2007 have been obtained without filter (W for white). We calibrate them against R-band, which, in in the case of no color evolution of the optical counterpart, is expected to result in a small constant offset in magnitude.

3.3 Real Time GRB followup

BOOTES-1B could have received during the past 4 years (since January 2005 until December 2008) 86 GRB triggers via GCN, which could have been followed in real time or would become observable within the following two hours. Table 6 summarizes these triggers, noting, among BOOTES-1B status of the followup, also the brightness of the GRB optical counterpart, if it is known. The magnitude estimation search was done with a heavy use of GRBlog [6]. We use these data to construct a "limiting magnitude vs. likelihood of detection" graph (Fig. 14).

3.3.1 GRB triggers followed by BOOTES-1B

GRB 050215B GRB was discovered by *Swift*/BAT at 02:33:43.2 UT. BOOTES received the notice, but because of a software error waited with the slew until ~22 minutes after the GRB. We coadded 600 s exposures taken by both 20 cm telescopes to obtain limits of V>16.5 and I>15.0 [7].

GRB 050505 First image of this *Swift*-discovered GRB [8] was obtained at 23:32:30 UT, i.e. 609 s after the trigger and 70 s after receiving the coordinates. No optical afterglow was detected [9].

GRB 050509A At the time of this trigger, the dome was still operating independently on the rest of the system - we obtained the first image 23 s after the GRB trigger (6 s after receiving the alert). The dome was closed due to what we consider a false trigger on the rain sensor. The first useful 10 s exposure was obtained 63.8 min after the burst and has a limiting magnitude of V>14.9. A coadd of first 112×10 s exposures with an exposure mean time 88.0 min after the GRB has a limit of V>18.1.

GRB 050509B This was a *Swift*-detected short gamma-ray burst [10]. Starting 62 s after the trigger, BOOTES-1B seems to have obtained the world-first data set of this short duration GRB. However, bad luck caused that the location of the GRB on the sky coincided with the tip of a nearby antenna and it's signalling light. The limiting magnitude is thus seriously degraded. The first 10 s exposure has a limiting magnitude V > 11.5, a combination of the first 12×10 s exposures provides V>12.5.

GRB 050525A GRB 050525A [11] was the first BOOTES-1B burst for which a detection was obtained. The telescope started the first exposure 383 s after the GRB trigger (28 s after receiving the notice). An optical afterglow with V≃15.0 was detected.

GRB 050528 We observed the errorbox [12] at 04:07:56 UT, ie. starting 71 s after the burst and 28 s after receiving the trigger in a light twilight, setting the limit to the possible GRB counterpart to V>13.8 and I>13.0 during the first 60 s after the beginning of our observation [13].

GRB 050730 Located at 19:58:23 UT, this GRB was very low above horizon in real time, BOOTES-1B obtained few exposures starting 233.4 s after the GRB, when the system failed. The images did not provide detection of the 17.0 mag optical transient discovered by both *Swift*/UVOT [14] and 1.5 m telescope at OSN [15].

GRB 050805B This short burst was localized by *Swift* at 20:41:26 UT, BOOTES obtained first images 62.2 s after the trigger (7.2 s after receiving the trigger). No optical transient was detected. The first 10 s exposure has a limiting magnitude R>16, combination of first five images (exposure mean time 118 s after the GRB) has a limit R>17.0.

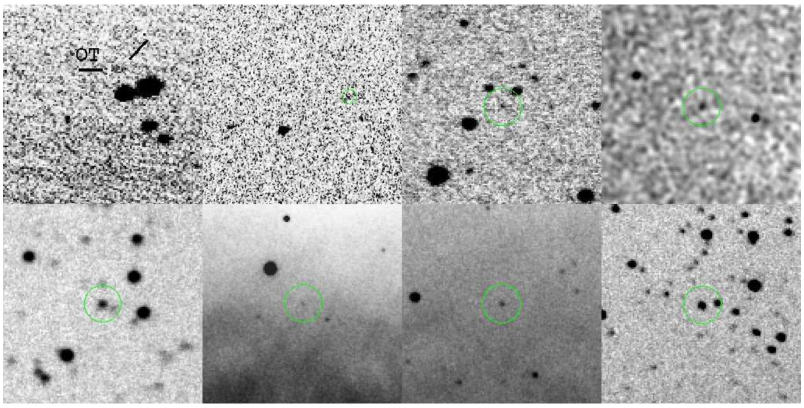

Figure 13: GRB optical transient detections by BOOTES-1B: first row: GRB 050824, GRB 050922C, GRB 051109A, GRB 080330. Second row: GRB 080413B, GRB 080430, GRB 080602B, GRB 080605.

GRB 050824 The optical afterglow of this GRB was discovered with the 1.5 m telescope at Sierra Nevada [16, 17]. BOOTES-1B was, however, the first telescope to observe this optical transient, starting 636 s after the trigger with R$\simeq$ 17.5. The weather was not stable and the focus not perfect, but BOOTES-1B worked as expected. Eventually, several hours of data were obtained.

GRB050904 BOOTES-1B reacted to this GRB, starting 124 s after the trigger. There was a hot pixel close to the GRB location, which made us believe we might have a detection in the *R*-band, which was issued in the first BOOTES-1B circular. Later, the observation revised as a limit (R>18.2) which was used to compute the record redshift of this GRB [18]. The I-band camera of the 20 cm telescope, unluckily, failed.

GRB 050922C This bright burst was detected by *Swift*/BAT at 19:55:50 UT. BOOTES was not very lucky - the weather on the station was bad. Instead of a limiting magnitude of ~ 17.0 for a 30 s exposure we got 12.9. The afterglow was eventually detected with the R-band camera (at the 30 cm telescope) on few occasions between flying clouds. The first weak detection was obtained 228 s after the GRB trigger gave R$\simeq$14.5.

GRB 051109A This is the only GRB ever detected by BOOTES-1B simultaneously in more than one filter. The first images were obtained 54.8 s after the burst in R and I bands [19].

GRB 051211B Observation of this burst started 42 s after the burst. A 30 s R-band exposure was obtained, but the camera failed after getting this image. Only useless defocused I-band images were taken with the 20 cm telescope [20].

GRB 051221B This GRB was detected by *Swift*/BAT at 20:06:48 UT [21]. BOOTES-1B slewed to the position and started obtaining images 27.8 s after receiving the alert (234.8 s after the burst). We did not find any new source in our images [22]. 30 min after the trigger, a faint 21 magnitude afterglow was discovered elsewhere [23].

GRB 060421 BOOTES-1B reacted to this GRB within 61 s after the trigger. Images were not of a great quality, yielding a limit of R>14 for the first 10 s exposure and R>16 for the combination of 30 images (exposure mean time 547 s after the trigger).

GRB 061110B The GRB was detected by *Swift*/BAT at T_0 =21:58:45 UT, but the notices were delayed by 626 s because *Swift* was performing downlink. BOOTES-1B started to slew immediately after reception of the trigger, obtaining the first image 698 s after the burst (72 s after the GCN notice). When seven 60 s exposures were obtained, a communication error with the mount occurred. The communication was later restored and further 19 images were obtained starting 22:49:49 UT (0.85 h after burst). Last image was obtained at 23:36:20 (1.62 h after burst).

Combination of the first 7 images (limiting magnitude ~17.2 mag each) with the exposure mean time 938 s after the GRB trigger was found to have a magnitude limit ~18.0. Combination of 11 images obtained between 22:49:49 UT and 23:03:45 UT (lim ~ 16.9 mag each) yields a limit of ~18.2 with mean time T_0+3452 s.

GRB 071101 First successful followup of a GRB after installation of the 30 cm telescope in BOOTES-2 site at La Mayora. The GRB trigger [24] was at 17:53:46 UT. BOOTES started imaging 54.8 s after the burst (23.3 s after receiving the coordinates). No afterglow was detected, an unfiltered, R-band calibrated limit of W>17.0 was estimated [25].

GRB 071109 *INTEGRAL* detected this GRB at 20:36:05 UT [26]. BOOTES followed up 58.5 s after the GRB (30.9 s after receiving the alert). Because of high altitude clouds, the telescope performance was reduced, yielding an unfiltered limit of ~13.0 in the first 10 s exposure [27].

GRB 080330 This GRB [28] happened during the first day recomissioning of BOOTES-1B after its move from BOOTES-2 site in La Mayora. The GCN client was not yet operational and at the time of the GRB we were focusing the telescope. First image was obtained 379 s after the GRB trigger and the optical afterglow was detected with magnitude ~16.3 on the first image. A bug in the centering algorithm caused a loss of part subsequent data. Further detections were obtained starting 21 min after the GRB when the problem was fixed.

GRB 080413A BOOTES-1B started obtaining images of the GRB 080413A [29] starting 60.7 s after the trigger (46.3 s after reception of the alert). A W≃13.3 magnitude optical afterglow was found [30].

GRB 080430 BOOTES-1B obtained the first image of this GRB [31] 34.4 s after the trigger. An optical transient was found with a magnitude W ≃ 15.5 [32].

GRB 080603B This GRB happened at BOOTES-1 site during sunset. We obtained first useful images starting one hour after the trigger. An W ≃ 17.4 optical transient was found.

GRB 080605 GRB 080605 was observed starting 41.9 s after the trigger. A rapidly decaying optical afterglow with W ≃ 14.8 was found [33].

GRB	$T_{obs} - T_{trigger}$	$T_{obs} - T_{notice}$	mag
050215B	22 min		V>16.5, I>15.0
050505	609 s	70 s	V>14.0
050509A	63.8 min		V>18.1
050509B	62 s	48 s	V>12.5
050525A	383 s	28 s	V≃15.0
050528	71 s	28 s	V>13.8, I>13.0
050730	233 s	172 s	R>16
050824	636 s	55.8 s	R≃17.5
050805B	62 s	17 s	R>16.0
050904	124 s	43 s	R>18.2
050922C	228 s	62.3 s	R≃14.5
051109A	54.8 s	27 s	R≃16.2
051211B	42 s	48.4 s	I>14.0
051221B	234.8 s	27.8 s	V>13.3
060421	61.2 s	47.6 s	R>16.0
061110B	698 s	72 s	R>18.0
071101	54.8 s	23.3 s	W>17.0
071109	58.5 s	30.9 s	W>13.0
080330	379 s		W≃16.3
080413A	60.7 s	46.3 s	W≃13.3
080430	34.4 s	22.1 s	W≃15.5
080603B	60 min		W≃17.4
080605	41.9 s	29.3 s	W≃14.8
081003	41 s	17.4 s	W>14.8

Table 4: Summary of GRBs successfully followed by BOOTES-1B.

GRB 081003B *INTEGRAL* detected this GRB at 20:36:05 UT [34]. BOOTES started obtaining unfiltered images at 20:48:49 UT (41 s after the GRB trigger and 17.4 s after the GCN notice), single images have a detection limit of W > 14 mag. The combination of the first 32 images with an exposure mean time of 80 s after the GRB has a limit of W > 17.6 mag (calibrated against GSC2). Neither shows any new sources within the GRB errorbox [35].

3.4 Implications

3.4.1 Success rate

Of the 89 triggers, 45 were processed in realtime and observed if possible, in 44 cases the system could not respond. This makes the overall failure rate quite high (50 %). 29 triggers were, however, lost due to long-term failures resulting from the telescope being struck by lightning. 8 more triggers failed during first 6 months of operation, when the system was not yet fully stable and one was lost during maintenance (and followed manually). 6 triggers out of 47 (13 %) were lost unexpectedly during the 963 nights of telescope operation if we do not count the first semester of 2005.

3.4.2 Planning

When specifying the GRB follow-up needs, the number of nights (hours) spent observing GRBs has to be estimated. Under various follow-up strategies we may derive different results.

Due to various instrumental effects (like a passage through the South Atlantic Anomaly) related to the satellite *Swift*, an offset from the overall triggering statistic which would depend on a geographical location could be found.

In Table 6, the fourth column has the time in hours until the first set of the event location below 10° of altitude or until the Sun rises above -15° of altitude. For non-realtime events, this is the time the location spends on the night sky, for real-time triggers, it is the time between the trigger and the moment when the target becomes unobservable.

For a small telescope, we assume that once the GRB is real-time triggered, it is unlikely to detect it the following night (i.e. after ~24 h), so we assume the following simple follow-up strategy: Let the telescope observe the GRB once it becomes accessible for the first time (which is immediately for real-time triggers) and let it observe until the GRB sets or the night ends. Do not observe any further nights. Under the given assumptions we get the following observing needs (assuming perfect weather):

Real time triggers There have been 72 real time triggers during the studied 4 years, during their first nights they accumulated 202 hours.

So if we allow only real-time followable triggers to be observed, we would need ~ 18 triggers per year (once per 20 days) and on average 2.8 h (max. 8.0 h) of observing time per trigger, 50.5 h per year. Such a program would consume about 2 % of the telescope time.

Extended set In the extended set, we assume that GRBs that would become observable within 2 hours after the event would also be followed. We would need ~22 triggers per year, each with an average length of 3.5 h. In total we would need 78.5 h per year, or about 3 % of the telescope time.

	Real time only	Up to 2 h
triggers/year	18	22
hours/year	50.5	78.5
hours/trigger	2.8	3.5
days/trigger	20.3	16.6

Table 5: Results of the GRB-planning statistic

3.4.3 Optical Afterglow Brightnesses

As a representative value of GRB optical transient brightness, important for real-time follow-up, we have chosen its magnitude at 300 s after the trigger. It turns out that it is not easy to find a uniform sample and available magnitudes and limits are a mixture of different passbands, mainly V,R and unfiltered CCD magnitudes. For a general idea of how bright an OT could be this is, however, good enough. Fig. 14 shows a cumulative probability of detecting an OT five minutes after the trigger with a telescope able to

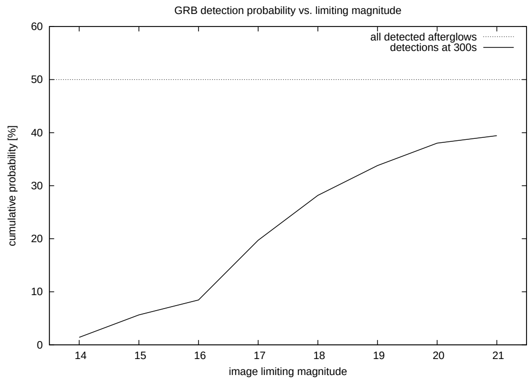

Figure 14: The graph (based on T_{300} data from Table 6), showing the likelihood of detection of an optical afterglow of a GRB as a function of the magnitude the telescope can detect (in the time interval discussed here). The dotted line delimits 50 % — the ratio of GRBs in our data for whose there was eventually discovered an optical transient.

detect a given magnitude. For many GRBs the brightness at this early time is unknown, or only a limit from small telescopes has been established, so this curve is actually a slight underestimation.

For example BOOTES-1B, which could detect mag ~ 18 at an unfiltered 60 s exposure, may detect an OT in about one third of the GRB triggers.

3.5 Conclusions

We have shown in a small historical retrospective the evolution of the telescope of BOOTES-1B, as it developed from the wide-field survey telescope to a dedicated GRB follow-up telescope.

Four years of BOOTES-1B GRB follow-up history are summarised for the first time transparently in the form of a table, which includes not only the observation status of BOOTES-1B, but also the time for which the object could have been observed, and a magnitude (or a limit) of the GRB optical afterglow 5 minutes after the trigger found in the literature. Every existing GRB trigger which was, or could have been observed by BOOTES-1B within 2 hours after the trigger is included. Twenty four successfully followed events are described case by case in a separate chapter. Many of these are published for the first time.

The data collected are also used to show the GRB trigger rate in Spain. By simply counting the triggers and the days during which they were collected, we estimate 18 triggers and about 50.5 h of telescope time per year for real time triggers. These numbers grow to about 22 triggers and 78.5 h per year if we include also the GRBs observable within 2 hours after the trigger. We also derive the likelihood of the optical afterglow detection five minutes after the GRB trigger depending on the limiting magnitude of the telescope.

Object	Target	t_1[h]	t_{obs}[h]	m_{300}[mag]	dT	observation status
050128	-	+0.0	1.8	-	-	No link to GCN
050208	-	+0.0	4.2	-	-	No link to GCN

050215B	5064	+0.4	10.0	≳ 16†[36]	22 m	V,I limits [7]
050306	5075	+0.2	1.8	>16[37]	86 s	w/roof closed
050416B	5109	+0.0	2.8	-	-	`grbd` failure
050421	5112	+0.0	0.2	>18.4 [38]	-	hw problems
050502A	-	+0.0	1.8	16.3[39]	-	`grbd` failure
050505	5123	+0.0	2.2	-†	609 s	clouds, V,I limits
050509A	5129	+0.0	2.2	>18.2[40]	23 s	hw problems, later limit
050509B	5130	+0.0	0.0	>20.8[41]	62 s	OK, $V > 12.5$, antenna hit!
050520	-	+0.0	3.6	>16.6	-	GCN connection lost
050525A	5136	+0.0	3.6	14.7[42]	383 s	OK, V-band lightcurve
050714A	1037	+0.0	3.6	-†	10 m	manually, later limit
050730	50008	+1.2	1.6	17.4[14]	1 h 40 m	limits
050805B	50015	+0.2	7.2	-	62 s	limits
050824	50032	+0.0	5.2	17.5[17]	636 s	detection [17]
050904	50055	+0.0	2.8	-†	124 s	R-band limit [18]
050922C	50090	+0.0	6.2	15.5[44]	228 s	detections between clouds
051109A	50126	+0.0	1.4	16.8	54.8 s	detection in R,I
051111	-	+0.0	4.6	14.9[45]	-	GCN connection lost
051211A	50144	+0.0	3.2	-†	-	CCD failure
051211B	50146	+0.0	4.8	>14.0	50 s	OK, limits [20]
051221B	50151	+0.0	3.8	>18.2[46]	235 s	OK, limits [22]
051227	50155	+1.6	10.6	>19.2[47]	59 m	bad weather
060111A	50162	+0.0	2.0	> 18.3[48]	296 s	during maintenance, limit
060121	-	+0.0	7.8	-†	-	telescope OFF
060123	50171	+0.0	7.6	-	-	bad weather
060130	50173	+0.0	1.2	-	-	bad weather
060203	-	+0.0	6.2	-	-	bad weather+no GCN
060204C	-	+0.0	9.6	> 18.7[49]	-	bad weather+no GCN
060206	-	+0.0	1.4	16.5[50]	-	GCN connection lost
060219	50185	+1.0	6.0	>18.6[51]	-	bad weather
060319	50190	+0.0	4.4	>19†[52]	-	bad weather
060418	50207	+0.0	1.4	14.2[53]	-	bad weather
060421	50208	+0.0	3.8	>16.8[54]	61.2 s	limit
060424	-	+0.0	0.0	-†	-	hw failure
060502A	-	+0.0	1.0	18.7[55]	-	hw failure
060507	-	+0.0	2.0	> 15.5†[56]	-	hw failure
060512	-	+0.0	4.6	17.15[57]	-	hw failure
060515	-	+0.0	1.4	>16.2[58]	-	hw failure
060522	-	+0.0	1.6	19.65[59]	-	hw failure
060602A	-	+0.0	1.2	>15†[60]	-	hw failure
060602B	-	+0.0	3.6	-	-	hw failure
060712	-	+0.2	3.0	> 14.5[61]	-	hw failure
060814	-	+0.0	0.8	>17.4[62]	-	hw failure
060825	-	+0.0	1.4	>18.3[63]	-	hw failure
060901	-	+1.6	5.2	-†	-	hw failure
060904A	-	+0.0	0.2	>19.5[64]	-	hw failure
060904B	-	+0.0	2.2	~17[65, 66]	-	hw failure
060929	50212	+0.0	1.2	>17.0[67]	-	bad weather
061019	50220	+0.0	1.0	>14.8†[68]	-	bad weather
061110B	50228	+0.0	2.2	>17.8†[69]	11 m38 s	> 18.1 OK
061217	50240	+0.0	2.6	>19.2 [70]	-	mount failure
061218	50242	+0.0	2.0	>18.6 [71]	-	mount failure
061222B	50245	+0.0	0.6	18.0 [72]	-	mount failure
070103	50246	+0.0	2.8	>19.6 [73]	-	mount failure
070129	50253	+0.0	0.4	>19.2†[74]	-	mount failure

070219	-	+0.0	4.8	>20.0 [75]	-	mount failure
070220	50258	+0.0	1.2	>19.6 [76]	-	mount failure
070223	50259	+0.0	4.6	>21.4† [77]	-	mount failure
070224	50260	+1.4	8.0	>20.1† [78]	-	mount failure
070406	50277	+0.0	4.0	-	-	mount failure
070411	-	+0.0	3.2	~18.3[79]	-	mount failure
070412	-	+0.0	3.2	>20.7[80]	-	mount failure
070429A	50286	+1.6	1.0	>18.0[81]	-	mount failure
070531	-	+0.0	1.4	>19.9[82]	-	mount failure
070610	-	+0.4	6.2	~19[83]	-	mount failure
070704	-	+1.4	6.2	>21.2 [84]	-	manually disabled
070714A	50010	+0.0	1.0	-†	52 s	bad weather
071025	50033	+0.0	0.4	17.3[85]	-	bad weather
071101	50038	+1.0	10.6	>19.7[86]	56 s	limit[25]
071109	50040	+0.0	1.0	>15.5[87]	59 s	thick cirrus, limit [27]
071112C	50044	+0.4	11.0	17.5[88]	64 s	bad weather
080320	50076	+0.0	0.6	>20[89]	-	bad weather
080330	50079	+0.0	1.2	16.8[90]	400 s	manual, detection
080413A	50082	+0.0	1.6	15.0	60.7 s	detection [29]
080430	50090	+0.8	7.4	17.5	34 s	detection [31] [32]
080517	50098	+0.0	2.4	>18.5[91]	3 h 22 m	weather delay
080603B	50113	+1.6	6.4	16.5[92]	1 h 15 m	detection
080605	50115	+0.0	3.8	17.9[93]	43 s	detection [33]
080727C	-	+0.0	4.8	>19.9[94]	-	dome failure
080903	-	+0.0	4.4	19.2[95]	-	dome failure
081001	50159	+0.0	1.4	-	-	bad weather
081003B	50167	+0.0	3.6	>17.6[35]	41 s	OK, limit [35]
081126	50181	+0.0	4.0	>18.0[96]	-	bad weather
081128A	50184	+1.2	9.8	20.9[97]	-	bad weather
081210	50188	+0.0	8.0	19.9[98]	45 m	weather delay, out of focus
081228	50195	+0.0	2.0	19.8[99]	-	bad weather
081230	50197	+0.0	3.2	19.1[100]	-	bad weather

Table 6: The Great Table of BOOTES-1B GRBs. "Target" is the RTS2 target number at BOOTES-1B. t_1 is the time delay between the GRB trigger and the possible start of observation. t_{obs} is the amount of time for which the GRB can be followed until it sets for the first time. m_{300} is the known brightness of the GRB optical transient 300 s after the event. dT is the delay of BOOTES-1B followup.
† denotes discovered optical counterparts where there are not enough data to estimate the brightness 300 s after the GRB.

References

[1] Castro-Tirado, A.J. et al., A&A Supl. Ser. 138, p.583, 1999

[2] Castro-Tirado A.J. et al., AN 325, 679, 2004

[3] Kubánek, P. et al., SPIE Conference Series, vol. 6274, 2006.

[4] Castro-Tirado A.J. et al., A&A 393, L55, 2000

[5] de Ugarte Postigo, A., Ph.D. Thesis, Univ. de Granada, 2007

[6] Quimby, R. et al., astro-ph/0312314v1, 2003

[7] Jelínek, M. et al., GCN Circ. 3023, 2005

[8] Hurkett, C. et al, GCN Circ. 3360, 2005

[9] de Ugarte Postigo, A. et al., GCN Circ. 3376, 2005

[10] Castro-Tirado et al., A&A 439, L15, 2005

[11] Band, D., GCN Circ. 3466, 2005

[12] Holland, S. T., GCN Circ. 3496, 2005

[13] Jelínek, M. et al., GCN Circ. 3500, 2005

[14] Blustin, A.J. et al., GCN Circ. 3717, 2005

[15] Pandey, S. et al., A&A 460, 415, 2006

[16] Gorosabel, J. et al., GCN Circ. 3866, 2005

[17] Sollerman, J. , A&A 466, 839-846, 2007

[18] Haislip, J.B. et al., Nature 440, 181-183, 2006

[19] Jelínek M., et al., GCN Circ. 4227, 2005

[20] Jelínek, M. et al., GCN Circ. 4333, 2005

[21] Boyd, P. et al., GCN Circ. 4376, 2005

[22] de Ugarte Postigo, A. et al., GCN Circ. 4379, 2005

[23] Halpern, J.P. & Tyagi, S., GCN Circ. 4381, 2005

[24] McBreen, S. et al., GCN Circ. 7030, 2007

[25] Jelínek, M. et al., GCN Circ. 7032, 2007

[26] Mereghetti, S. et al., GCN Circ. 7046, 2007

[27] de Ugarte Postigo, A. et al., GCN Circ. 7047, 2007

[28] Mao, J. et al., GCN Circ. 7537, 2008

[29] Kubánek, P. et al., GCN Circ. 7603, 2008

[30] Jelínek, M et al., in preparation

[31] Jelínek, M. et al., GCN Circ. 7648, 2008

[32] de Ugarte Postigo, A. et al., in preparation

[33] Jelínek, M. et al., GCN Circ. 7837, 2008

[34] Gotz, D. et al., GCN Circ. 8317, 2008

[35] Jelínek, M. et al., GCN Circ. 8320, 2008

[36] Yost, S.A. et al., GCN Circ. 3022, 2005

[37] Quimby R.M. et al., GCN Circ. 3107, 2005

[38] Rykoff, E.S. et al., GCN Circ. 3304, 2005

[39] Guidorzi, C. et al., APJ 630, L121-L124, 2005

[40] Poole, T. et al., GCN Circ. 3394, 2005

[41] Wozniak, P. et al., GCN Circ. 3414, 2005

[42] Blustin, A.J. et al., ApJ 637, 901, 2006

[43] Monfardini, A. et al., GCN Circ. 3497, 2005

[44] D. Hunsberger, S.D. et al, GCN Circ. 4041, 2005

[45] Mundell, C.G. et al, GCN Circ. 4250, 2005

[46] Klotz, A. et al., GCN Circ. 4386, 2005

[47] Roming, P. et al., GCN Circ. 4411, 2005

[48] Klotz, A. et al., GCN Circ. 4483, 2006

[49] Melandri, A. et al., GCN Circ. 4665, 2006

[50] Guidorzi, C. et al., GCN Circ. 4693, 2006

[51] Breeveld, A. & Moretti, A., GCN Circ. 4798, 2006

[52] Melandri, A. et al., GCN Circ. 4889, 2006

[53] Jelínek, M. et al., GCN Circ. 4976, 2006

[54] Lipunov, V. et al., GCN Circ. 4988, 2006

[55] Poole, T. S, & La Parola, V., GCN Circ. 5068, 2006

[56] Jelinek, M., et al., GCN Circ. 5092, 2006

[57] Pasquale, M. D, & Cummings, J.,GCN Circ. 5130, 2006

[58] Klotz, A., Boer, M., & Atteia, J. L, GCN Circ. 5134, 2006

[59] Holland, S. T., GCN Circ. 5158, 2006

[60] Vítek, S., et al., GCN Circ. 5201, 2006

[61] Lipunov, V., et al., GCN Circ. 5303, 2006

[62] Klotz, A., Boer, M., & Atteia, J. L, GCN Circ. 5448, 2006

[63] Gomboc, A., GCN Circ. 5476, 2006

[64] Klotz, A., Boer, M., & Atteia, J. L, GCN Circ. 5506, 2006

[65] Rykoff, E. S. et al, ApJ, 2009 [astro-ph/0904.0261]

[66] Jelínek, M. et al., in preparation, 2009

[67] Nekola, M. et al., GCN Circ. 5658, 2006

[68] Klotz, A. et al., GCN Circ. 5731, 2006

[69] Mikuz, H., GCN Circ. 5808, 2006

[70] Klotz, A. et al, GCN Circ. 5942, 2006

[71] D'Avanzo, P. et al, GCN Circ. 5937, 2006

[72] de Ugarte Postigo, A. et al, GCN Circ. 5968, 2006

[73] Holland, S. T. & Sakamoto, T., GCN Circ. 5993, 2006

[74] Chester, M. M. & Godet, O., GCN Circ. 6066, 2007

[75] Breeveld, A. & Sakamoto, T., GCN Circ. 6111, 2007

[76] Stamatikos, M. et al., GCN Circ. 6114, 2007

[77] Landsman, W. et al., GCN Circ. 6134, 2007

[78] Holland, S. T. et al., GCN Circ. 6152, 2007

[79] Mikuz, H. et al., GCN Circ. 6288, 2007

[80] Mikuz, H. & Dintinjana B., GCN Circ. 6284, 2007

[81] Rykoff, E. S. et al., GCN Circ. 6356, 2007

[82] de Pasquale, M. & Markwardt, C.B., GCN Circ. 6481, 2007

[83] Stefanescu, A., et al. GCN Circ. 6492, 2007

[84] Meshcheryakov, A., et al, GCN Circ. 6617, 2007

[85] Rykoff, E.S. et al., GCN Circ. 6992, 2007

[86] Uemura, M. et al., GCN Circ. 7037, 2007

[87] Klotz, A. et al., GCN Circ. 7052, 2007

[88] Dintinjana, B. et al., GCN Circ. 7078, 2007

[89] Williams, G.G. & Milne, P.A., GCN Circ. 7492, 2008

[90] Klotz, A. et al., GCN Circ. 7543, 2008

[91] Parsons, A.M. et al., GCN Circ. 7742, 2008

[92] Kuin, N.P.M. et al., GCN Circ. 7808, 2008

[93] Rumyantsev, V. et al., GCN Circ. 7833, 2008

[94] Hoversten, E. A. & Parsons, A. M., GCN Circ. 8043, 2008

[95] Marshall, F.E. et al., GCN Circ. 8179, 2008

[96] Gendre, B. et al., GCN Circ. 8555, 2008

[97] Xin L.P. et al., GCN Circ. 8572, 2008

[98] Immler, S. et al., GCN Circ. 8654, 2008

[99] Afonso, P. et al., GCN Circ. 8752, 2008

[100] Yuan, F. et al., GCN Circ. 8754, 2008